



UNIVERSITÀ POLITECNICA DELLE MARCHE
Repository ISTITUZIONALE

Ostreopsis fattorussoi sp. nov. (Dinophyceae), a new benthic toxic *Ostreopsis* species from the eastern Mediterranean Sea.

This is the peer reviewed version of the following article:

Original

Ostreopsis fattorussoi sp. nov. (Dinophyceae), a new benthic toxic *Ostreopsis* species from the eastern Mediterranean Sea / Accoroni, Stefano; Romagnoli, Tiziana; Penna, A.; Capellacci, S.; Ciminiello, P.; Dell'Aversano, C.; Tartaglione, L.; Abboud Abi Saab, M.; Giussani, V.; Asnaghi, V.; Chiantore, M.; Totti, Cecilia Maria. - In: JOURNAL OF PHYCOLOGY. - ISSN 1529-8817. - 52:(2016), pp. 1064-1084. [10.1111/jpy.12464]

Availability:

This version is available at: 11566/245056 since: 2022-06-01T12:50:56Z

Publisher:

Published

DOI:10.1111/jpy.12464

Terms of use:

The terms and conditions for the reuse of this version of the manuscript are specified in the publishing policy. The use of copyrighted works requires the consent of the rights' holder (author or publisher). Works made available under a Creative Commons license or a Publisher's custom-made license can be used according to the terms and conditions contained therein. See editor's website for further information and terms and conditions.

This item was downloaded from IRIS Università Politecnica delle Marche (<https://iris.univpm.it>). When citing, please refer to the published version.

note finali coverpage

(Article begins on next page)

WILEY

Online Proofing System Instructions

The Wiley Online Proofing System allows authors and proof reviewers to review PDF proofs, mark corrections, respond to queries, upload replacement figures, and submit these changes directly from the PDF proof from the locally saved file or while viewing it in your web browser.

1. For the best experience reviewing your proof in the Wiley Online Proofing System please ensure you are connected to the internet. This will allow the PDF proof to connect to the central Wiley Online Proofing System server. If you are connected to the Wiley Online Proofing System server you should see the icon with a green check mark above in the yellow banner.



Connected



Disconnected

2. Please review the article proof on the following pages and mark any corrections, changes, and query responses using the Annotation Tools outlined on the next 2 pages.



3. To save your proof corrections, click the “Publish Comments” button appearing above in the yellow banner. Publishing your comments saves your corrections to the Wiley Online Proofing System server. Corrections don’t have to be marked in one sitting, you can publish corrections and log back in at a later time to add more before you click the “Complete Proof Review” button below.



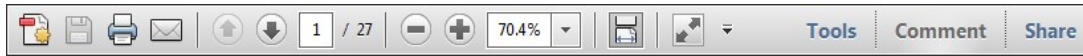
4. If you need to supply additional or replacement files bigger than 5 Megabytes (MB) do not attach them directly to the PDF Proof, please click the “Upload Files” button to upload files:

5. When your proof review is complete and you are ready to submit corrections to the publisher, please click the “Complete Proof Review” button below:

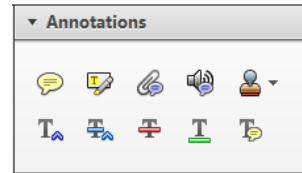
IMPORTANT: Do not click the “Complete Proof Review” button without replying to all author queries found on the last page of your proof. Incomplete proof reviews will cause a delay in publication.

IMPORTANT: Once you click “Complete Proof Review” you will not be able to publish further corrections.

Once you have Acrobat Reader open on your computer, click on the [Comment](#) tab at the right of the toolbar:



This will open up a panel down the right side of the document. The majority of tools you will use for annotating your proof will be in the [Annotations](#) section, pictured opposite. We've picked out some of these tools below:



1. Replace (Ins) Tool – for replacing text.

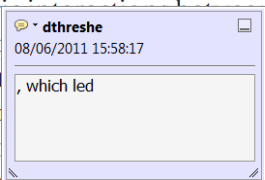


Strikes a line through text and opens up a text box where replacement text can be entered.

How to use it

- Highlight a word or sentence.
- Click on the [Replace \(Ins\)](#) icon in the Annotations section.
- Type the replacement text into the blue box that appears.

standard framework for the analysis of microeconomic activity. Nevertheless, it also led to the development of a new paradigm of strategic behavior. The number of competitors in the industry is that the structure of the industry is a main component. At the industry level, are externalities important? (M henceforth) we open the 'black b



2. Strikethrough (Del) Tool – for deleting text.



Strikes a red line through text that is to be deleted.

How to use it

- Highlight a word or sentence.
- Click on the [Strikethrough \(Del\)](#) icon in the Annotations section.

there is no room for extra profits as mark-ups are zero and the number of firms (net) values are not determined by market clearing. Blanchard and ~~Kiyotaki~~ (1987), perfect competition in general equilibrium. The effects of aggregate demand and supply shocks in the classical framework assuming monopolistic competition. An exogenous number of firms

3. Add note to text Tool – for highlighting a section to be changed to bold or italic.



Highlights text in yellow and opens up a text box where comments can be entered.

How to use it

- Highlight the relevant section of text.
- Click on the [Add note to text](#) icon in the Annotations section.
- Type instruction on what should be changed regarding the text into the yellow box that appears.

dynamic responses of mark-ups consistent with the VAR evidence

sation by Markov processes. The number of competitors and the impact on the structure of the sector is that the structure of the sector



4. Add sticky note Tool – for making notes at specific points in the text.



Marks a point in the proof where a comment needs to be highlighted.

How to use it

- Click on the [Add sticky note](#) icon in the Annotations section.
- Click at the point in the proof where the comment should be inserted.
- Type the comment into the yellow box that appears.

and supply shocks. Most of the time, the number of competitors and the impact on the structure of the sector is that the structure of the sector



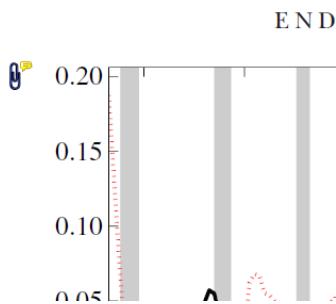
5. Attach File Tool – for inserting large amounts of text or replacement figures.



Inserts an icon linking to the attached file in the appropriate place in the text.

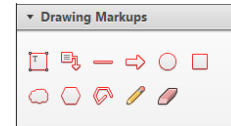
How to use it

- Click on the **Attach File** icon in the Annotations section.
- Click on the proof to where you'd like the attached file to be linked.
- Select the file to be attached from your computer or network.
- Select the colour and type of icon that will appear in the proof. Click OK.



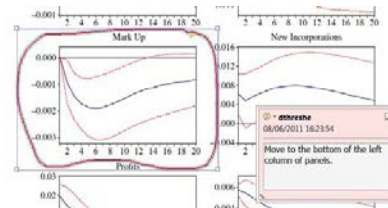
6. Drawing Markups Tools – for drawing shapes, lines and freeform annotations on proofs and commenting on these marks.

Allows shapes, lines and freeform annotations to be drawn on proofs and for comment to be made on these marks.



How to use it

- Click on one of the shapes in the Drawing Markups section.
- Click on the proof at the relevant point and draw the selected shape with the cursor.
- To add a comment to the drawn shape, move the cursor over the shape until an arrowhead appears.
- Double click on the shape and type any text in the red box that appears.



OSTREOPSIS FATTORUSSOI SP. NOV. (DINOPHYCEAE), A NEW BENTHIC TOXIC
OSTREOPSIS SPECIES FROM THE EASTERN MEDITERRANEAN SEA¹

Stefano Accoroni 

Dipartimento di Scienze della Vita e dell'Ambiente, Università Politecnica delle Marche, via Breccie Bianche, 60131 Ancona, Italy
 Consorzio Interuniversitario Scienze del Mare (CoNISMa), Via Flaminio 9, 00196 Roma, Italy

Tiziana Romagnoli

Dipartimento di Scienze della Vita e dell'Ambiente, Università Politecnica delle Marche, via Breccie Bianche, 60131 Ancona, Italy

Antonella Penna, Samuela Capellacci

Consorzio Interuniversitario Scienze del Mare (CoNISMa), Via Flaminio 9, 00196 Roma, Italy
 Dipartimento di Scienze Biomolecolari, Università di Urbino, Viale Trieste 296, 61100 Pesaro, Italy

Patrizia Ciminiello, Carmela Dell'Aversano, Luciana Tartaglione

Dipartimento di Farmacia, Università degli Studi di Napoli "Federico II", Via D. Montesano 49, 80131 Napoli, Italy

Marie Abboud-Abi Saab

National Council for Scientific Research/National Center for Marine Sciences, P.O. Box 534, Batroun, Lebanon

Valentina Giussani

Dipartimento di Scienze della Terra, dell'Ambiente e della Vita, Università degli Studi di Genova, Corso Europa 26, 16132 Genoa, Italy

Valentina Asnaghi, Mariachiara Chiantore

Consorzio Interuniversitario Scienze del Mare (CoNISMa), Via Flaminio 9, 00196 Roma, Italy
 Dipartimento di Scienze della Terra, dell'Ambiente e della Vita, Università degli Studi di Genova, Corso Europa 26, 16132 Genoa, Italy

and *Cecilia Totti*²

Dipartimento di Scienze della Vita e dell'Ambiente, Università Politecnica delle Marche, via Breccie Bianche, 60131 Ancona, Italy
 Consorzio Interuniversitario Scienze del Mare (CoNISMa), Via Flaminio 9, 00196 Roma, Italy

The new benthic toxic dinoflagellate *Ostreopsis fattorussoi* sp. nov. is described from eastern Mediterranean Sea Lebanon and Cyprus coasts, supported by morphological and molecular data. The plate formula, Po, 3', 7'', 6c, 7s, 5''', 2''''', is typical for the *Ostreopsis* genus. It differs from all other *Ostreopsis* species in that (i) the curved suture between plates 1' and 3' makes them approximately hexagonal, (ii) the 1' plate lies in the left-half of the epitheca and is obliquely orientated leading to a characteristic shape of plate 6''. The round thecal pores are bigger than the other two Mediterranean species (*O. cf. ovata* and *O. cf. siamensis*). *O. fattorussoi* is among the smallest species of the genus (DV: 60.07 ± 5.63 µm, AP: 25.66 ± 2.97 µm, W: 39.81 ± 5.05 µm) along with *O. ovata*. Phylogenetic analyses based on the LSU and

internal transcribed spacer rDNA shows that *O. fattorussoi* belongs to the Atlantic/Mediterranean *Ostreopsis* spp. clade separated from the other *Ostreopsis* species. *O. fattorussoi* produces OVTX-a and structural isomers OVTX-d and -e, *O. cf. ovata* is the only other species of this genus known to produce these toxins. The Lebanese *O. fattorussoi* did not produce the new palytoxin-like compounds (ovatoxin-i, ovatoxin-j₁, ovatoxin-j₂, and ovatoxin-k) that were previously found in *O. fattorussoi* from Cyprus. The toxin content was in the range of 0.28–0.94 pg · cell⁻¹. In Lebanon coast, *O. fattorussoi* was recorded throughout the year 2015 (temperature range 18°C–31.5°C), with peaks in June and August.

Key index words: benthic dinoflagellates; harmful algae; Mediterranean Sea; nutrients; *Ostreopsis*; ovatoxins; palytoxins; phylogeny; taxonomy

Abbreviations: AP, anterioposterior diameter; DV, dorsoventral diameter; ITS, internal transcribed

¹Received 12 May 2016. Accepted 2 August 2016.

²Author for correspondence: e-mail c.totti@univpm.it.
 Editorial Responsibility: R. Wetherbee (Associate Editor)

1 spacer; L:D, Light:Dark; LC-HR MSⁿ, Liquid Chromatography-High Resolution Multiple Stage Mass Spectrometry; ML, Maximum Likelihood; MP, Maximum Parsimony; NJ, Neighbor Joining; OVTX, ova-toxin; PLTX, palytoxins; RP, resolving power; UV, Ultraviolet; W, transdiameter

9 The genus *Ostreopsis* belongs to the family of
10 Ostreopsidaceae (Gonyaucales, Dinophyceae), which
11 includes two genera of benthic dinoflagellates (i.e.,
12 *Ostreopsis* and *Coolia*). The type species, *Ostreopsis si-*
13 *amensis* Schmidt was first described in the Gulf of
14 Siam (Thailand) in 1900 (Schmidt 1901). In the fol-
15 lowing years, several other species have been
16 described by other authors: *O. lenticularis* Fukuyo,
17 *O. ovata* Fukuyo (Fukuyo 1981), *O. heptagona* Norris,
18 Bomber & Balech (Norris et al. 1985), *O. mascaren-*
19 *ensis* Quod (Quod 1994), *O. labens* Faust & Morton
20 (Faust and Morton 1995), *O. marina* Faust, *O. be-*
21 *lizeana* Faust and *O. caribbeana* Faust (Faust 1999,
22 Hoppenrath et al. 2014). Of late, however, the valid-
23 ity of some *Ostreopsis* species has been questioned.
24 Although the taxonomy of *Ostreopsis* is based on
25 morphological characters (thecal plate pattern,
26 shape and size), high morphological variability is
27 reported within the same species and the original
28 descriptive characters of some species are often con-
29 sidered inadequate to discriminate among most
30 *Ostreopsis* species in field samples (Penna et al. 2005,
31 Parsons et al. 2012, David et al. 2013). In addition
32 to the confusion on the morphological features, no
33 genetic data were provided in these original descrip-
34 tions and the submission of any further new species
35 description accompanied by a sequence and com-
36 parison with other sequences in GenBank has been
37 recommended (Parsons et al. 2012). Lately, several
38 phylogenetic studies based on LSU and internal
39 transcribed spacer (ITS) analyses have been carried
40 out on *Ostreopsis* species, supplying an increasing
41 number of molecular clades (and subclades) that
42 may represent cryptic species (Penna et al. 2010,
43 2014, Sato et al. 2011, Tawong et al. 2014).

44 *Ostreopsis* species were reported since a long time
45 in tropical ciguatera endemic areas (Carlson and
46 Tindall 1985, Bomber and Aikman 1989) and were
47 often wrongly implicated in incidences of ciguateric
48 syndrome (e.g., Tosteson 1995). Indeed, some *Ostre-*
49 *opsis* species are toxic, but their toxins (mostly
50 belonging to the palytoxin group) are not those
51 that cause ciguatera. Among the nine species of the
52 genus *Ostreopsis*, toxicity has been demonstrated in
53 *O. siamensis* (also for *O. cf. siamensis*), *O. mascarenen-*
54 *sis*, *O. lenticularis* and *O. cf. ovata* (Nakajima et al.
55 1981, Yasumoto et al. 1987, Holmes et al. 1988,
56 Mercado et al. 1994, Meunier et al. 1997, Lenoir
57 et al. 2004, Ciminiello et al. 2006, Scalco et al.
58 2012, Uchida et al. 2013, García-Altare et al. 2014,
59 Brissard et al. 2015). Moreover, *O. heptagona* was
60 determined to be toxic, as methanol extracts of this

species isolated from Knight Key (Florida) were weakly toxic to mice (Babinchak, according to Norris et al. 1985).

In the past decade, *Ostreopsis* blooms have also become common also in temperate areas during the summer-autumn period (Chang et al. 2000, Rhodes et al. 2000, Pearce et al. 2001, Vila et al. 2001, Taniyama et al. 2003, Turki 2005, Aligizaki and Nikolaidis 2006, Mangialajo et al. 2008, Shears and Ross 2009, Totti et al. 2010, Illoul et al. 2012, Ismael and Halim 2012, Pfannkuchen et al. 2012, Selina et al. 2014). In these areas, *Ostreopsis* blooms are often associated with noxious effects on the health of humans (Tichadou et al. 2010, Del Favero et al. 2012) and benthic marine organisms (Accoroni et al. 2011, Pagliara and Caroppo 2012, Gorbi et al. 2013, Carella et al. 2015).

In the Mediterranean Sea, two genotypes corresponding to the morphotypes *O. cf. ovata* and *O. cf. siamensis* have been recorded to date (Penna et al. 2010, 2012). Almost all knowledge about the ecology of *Ostreopsis* species in the Mediterranean Sea mainly refers to *O. cf. ovata* due to its dominance over the other species in this area (Battocchi et al. 2010, Perini et al. 2011). Several environmental parameters have been recognized to strongly influence bloom dynamics, such as hydrodynamics, water temperature and nutrients (Vila et al. 2001, Shears and Ross 2009, Totti et al. 2010, Mabrouk et al. 2011, Mangialajo et al. 2011, Cohu et al. 2013).

The genotype *O. cf. siamensis* has been detected along the Catalan coast, in the eastern Atlantic coast of Morocco, Portugal, northern Spain and southern Italy (Vila et al. 2001, Amorim et al. 2010, Benouna et al. 2010, Laza-Martinez et al. 2011, Ciminiello et al. 2013, David et al. 2013) and its morphotype has also been reported along the Tunisian and Lebanese coasts (Turki 2005, Turki et al. 2006, Mabrouk et al. 2011, 2012, Abboud-Abi Saab et al. 2013). In addition to these two species, recently Penna et al. (2012) found a new genotype probably corresponding to a new species of *Ostreopsis*, in both the Atlantic Ocean (Canary Islands) and Mediterranean Sea (Greece and Cyprus Island). Strains of this new genotype collected in Cyprus have been reported to produce OVTX-a, -d, -e, and isobaric palytoxin, so far found only in *O. cf. ovata*, adding three new palytoxin-like compounds to those already identified, that is, OVTX-i, OVTX-j₁, OVTX-j₂, and OVTX-k (Tartaglione et al. 2015). This genotype will be described here as a new species.

Description of new species is often based on culture material rather than field samples (e.g., Litaker et al. 2009, Tillmann et al. 2009, Fraga et al. 2011, Percopo et al. 2013, Fraga and Rodríguez 2014). This approach, however, can have drawbacks when cells in culture strongly change their morphology producing aberrant cells and/or modifying the shape and the size of the thecal plates and the entire cell, as occurs in *Ostreopsis* (Aligizaki and

Nikolaidis 2006, Laza-Martinez et al. 2011, Nascimento et al. 2012, Scalco et al. 2012, David et al. 2013). Moreover, under certain culture conditions, in addition to the typical vegetative morphology, different stages of life cycle (characterized by different size, shape, and plate tabulation) may appear (Ali-gizaki and Nikolaidis 2006, Bravo et al. 2012, Accor-
 oni et al. 2014). On the other hand, the observation of culture material is necessary to obtain genetic material for gene sequencing and may be necessary to describe the whole range of morphological variability of a species and its different life stages in order to avoid diverse life stages of the same species being described as different species (Coats 2002). It is, therefore, crucial to use both culture and natural samples in the description of a new species.

In this study, we describe *Ostreopsis fattorussoi*, a new toxic benthic dinoflagellate found in the Lebanon and Cyprus coasts (eastern Mediterranean Sea), on the basis of molecular and ultrastructural features of both natural and culture samples. We also investigated the ecology of this new species along the Lebanon coast and analyzed its toxin content and profile.

MATERIALS AND METHODS

Sampling and sample treatment. Macroalgal samples were collected at three sites from Cyprus and Lebanon in 2013 and 2015, respectively: site 1, Vassiliko Bay, southern coast of Cyprus (34°43' 19.61" N, 33°18' 6.67" E), site 2, Batroun, Lebanon (34°15' 5.40" N, 35°39' 24.78" E), and site 3, Byblos, Lebanon (34°06' 51.84" N, 35°38' 53.76" E; Fig. 1). All sites were located in shallow and rocky shores.

Macroalgae (mainly *Halopteris scoparia* (Linnaeus) Sauvageau in Cyprus and *Corallina elongata* Ellis & Solander in Lebanon) were sampled and then processed to detach epiphytic cells (see below). Samples for microscope observations were fixed with 0.8% neutralized formaldehyde (Thronsen 1978) and stored at 4°C in the dark until the analyses.

At site 2 (Batroun, Lebanon), an ecological study about the temporal trend of *Ostreopsis* abundances and the

relationships with some environmental parameters was carried out. This site is characterized by rocky bottom and is affected by the discharge of phosphate into the sea from a chemical factory.

The sampling was carried out monthly from January to April 2015, then every 3–7 d until October 2015. The temperature was recorded using an alcohol thermometer (precision + 0.1°C). Salinity was measured using an induction salinometer (Beckman RS7-C) once back in laboratory. Surface water samples for nutrient analyses were collected through plastic bottles. Samples were immediately stored at –20°C. Orthophosphates (P-PO₄) were analyzed according to Murphy and Riley (1962), nitrites (N-NO₂) and nitrates (N-NO₃) to Strickland and Parsons (1968).

Macrophytes and seawater samples were collected in triplicate following the protocol of the ENPI-CBCMED project M3-HABS (<http://m3-habs.net>). Water samples were collected in plastic bottles (250 mL) at 20 cm depth (30 cm above the macroalgae), before the collection of the benthic substrata, in order to avoid resuspension. Portions of macroalgal thalli (~15 g) were collected using 250 mL plastic bottles. The seaweed samples in the storage water were shaken vigorously to dislodge the epiphytic cells, then the thalli were re-rinsed with filtered seawater to completely remove *Ostreopsis* cells. Finally, the samples were fixed by adding Lugol's solution at 1% V/V and stored at 4°C in the dark until the analyses.

Light microscope analysis. Light microscopy observations for the new species description were carried out using an inverted microscope (Zeiss Axiovert 135) equipped with phase contrast, differential interference contrast and epifluorescence with a UV lamp. Field samples were analyzed after staining with the DNA-specific dye SYBR Green to visualize the nucleus and the cellulose specific dye Calcofluor-White M2R to elucidate the thecal morphology.

Microphotographs were taken with a Canon EOS 6D (Canon Inc., Tokyo, Japan) digital camera. In the event that the field depth was not enough for the whole subject, multiple images taken at different focus distances were merged using image manipulation software.

Ostreopsis cells from field samples were measured at 400× magnification using a micrometric ocular. In samples of both Cyprus and Lebanon, 141 cells were measured along the dorsoventral diameter (DV) and the transdiameter (W); for a subset of cells (101) the anterioposterior diameter (AP) was also measured, using a needle to turn them over.

Abundances of *Ostreopsis* cells at site 2 were estimated both in benthic and in planktonic subsamples (1 and 50 mL, respectively) after homogenization. Counting was carried out in Utermöhl chambers (Edler and Elbrachter 2010) for seawater samples or Sedgewick-Rafter chambers (Guillard 1978) for benthic samples, through an inverted light microscope (Wild M40) and a light microscope, (Motic BA 400) respectively, both equipped with phase contrast, at 200× magnification. Counting was performed on random transects, or on the half chamber, in order to count a representative cell number. Cell abundances were expressed as cells · g⁻¹ fw and cells · L⁻¹ for water column.

Estimates of the net growth rates ($\mu \cdot d^{-1}$) of the natural populations of *Ostreopsis* throughout the year were calculated according to:

$$\mu = (\ln N_2 - \ln N_1) / (t_2 - t_1)$$

where N_2 and N_1 are *Ostreopsis* abundances on each benthic substrata at respective sampling day, t_1 , or t_2 .

The abundances of *Ostreopsis* in benthic samples were tested for significant correlations (Pearson) with all recorded environmental parameters and with abundance in the water

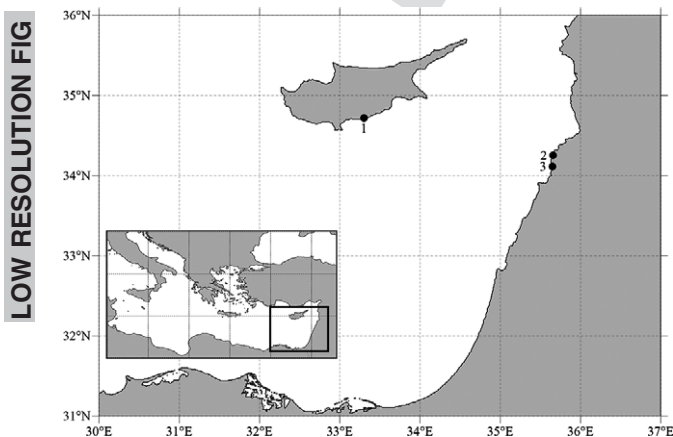


FIG. 1. Map of study area, showing the sites where *Ostreopsis fattorussoi* was found. Site 1: Vassiliko Bay (Cyprus). Site 2: Batroun (Lebanon). Site 3: Byblos (Lebanon).

1 column. Growth rates were tested for significant correlations
2 (Pearson) with all environmental parameters. The statistical
3 analyses were conducted using Statistica (Statsoft) software.

4 *Scanning electron microscope analysis.* Some preserved sub-
5 samples (1–5 mL) were dehydrated by immersion in ethanol
6 at increasing gradations (10%, 30%, 50%, 70%, 80%, 90%,
7 95%, and 100%). After 1 d in absolute ethanol, the dehy-
8 drated samples were filtered on a Nucleopore polycarbonate
9 filter, and treated in a Critical Point Dryer (Polaron CPD
10 7501). Filters were placed on stubs and sputtered with gold-
11 palladium in a Sputter Coater (Polaron SC 7640) for observa-
12 tion under the scanning electron microscopy (FE-SEM; Zeiss
13 Supra 40).

14 *Strain isolation.* *Ostreopsis* cell isolates were obtained from
15 microphytobenthos epiphytic on seaweeds collected on July
16 2013 and June 2014 at site 1, Vasiliko Bay (Cyprus), and site
17 2, Batroun (Lebanon), respectively, using the capillary pipette
18 method (Hoshaw and Rosowski 1973). After an initial growth
19 in microplates, cells were cultured at $23^{\circ}\text{C} \pm 1^{\circ}\text{C}$ under a
20 14:10 L:D photoperiod and an irradiance of $100 \mu\text{mol photons} \cdot \text{m}^{-2} \cdot \text{s}^{-1}$,
21 in modified f/10 medium Si free (Guillard 1975) using filtered and autoclaved natural seawater (salinity
22 35). One (C1005) and five (L1000, L1007, L1008, L1020, and
23 L1022) strains of *Ostreopsis* sp. were isolated from site 1 and
24 2, respectively (Table 1).

25 *DNA extraction, PCR amplification, sequence align-
26 ment.* Genomic DNA was extracted and purified from 50 mL
27 monoclonal cultures of *Ostreopsis* sp. in logarithmic growth
28 phase using a DNeasy Plant Kit (Qiagen, CA, USA) according to
29 the manufacturer's instructions. Briefly, cultures were col-
30 lected by centrifugation at $3,000 g$ for 20 min. The super-
31 natant was removed and the pellets were transferred to a 1.5-
32 mL tube, centrifuged at $13,000 g$ for 10 min. The pellets were
33 immediately processed or stored at -80°C until DNA extrac-
34 tion.

35 The PCR amplification of ribosomal 5.8S gene and non-
36 coding ITS regions, and partial nuclear LSU (D1/D2
37 domains) were described in Penna et al. (2010). Amplified
38 PCR fragments were purified (Penna et al. 2014) and sent to
39 Eurofins Genomics (Ebersberg, Germany). All nucleotide
40 sequences of ITS-5.8S rDNA and LSU deposited in ENA-
41 EMBL are listed in Table 1.

42 *Phylogenetic analyses.* The ITS-5.8S and LSU sequences
43 were aligned using MAFFT software. Short aligned sequences
44 and ambiguously aligned positions were excluded from the
45 alignment manually or using Gblocks
46 (<http://molevol.cmima.csic.es/castresana/Gblocks.html>) with
47 default settings.

48 The jModelTest v.2.1.7 (Darriba et al. 2012) was used to
49 determine the evolutionary model that best fitted data
50 according to Akaike Information Criterion. For both ITS-5.8S
51 and LSU gene rDNA alignment, the most appropriate evolu-
52 tionary model was found to be HKY+I+G with a gamma dis-
53 tributed rate of variation among sites equal to 1.56 and 1.47,
54 respectively.

55 Neighbor-Joining (NJ) and Maximum Parsimony (MP)
56 analyses were performed using MEGA6 (Tamura et al. 2013).
57 The MP analyses were performed using the Tree-Bisection-
58 Redrafting algorithm with search level 1 in which the initial
59 trees were obtained by the random addition of sequences (10
60 replicates). All positions containing gaps and missing data
were eliminated. The robustness of NJ and MP trees was
tested by bootstrapping using 1,000 pseudo-replicates. Maxi-
mum likelihood (ML) analyses were run with Phyml v.3.0
(Guindon et al. 2010). Bootstrap values were calculated with
1,000 pseudo-replicates.

Bayesian analyses (BI) were performed using MrBayes v.
3.2.3 (Ronquist and Huelsenbeck 2003) with the following

settings: four Markov chains were run for 2,000,000 genera-
tions with a sampling frequency of 100 generations. Log-likeli-
hood values for sampled trees were stabilized after almost
200,000 generations. The last 18,000 trees were used to esti-
mate Bayesian posterior probabilities, whereas the first 2001
were discarded as burn-in. Results from two-independent runs
were used to construct a majority-rule consensus tree contain-
ing the posterior probabilities.

The sequences of *Coolia monotis* VGO783 (FN256433) and
VGO786 (AM902737) were used as outgroups for the *Ostreop-
sis* ITS-5.8S and LSU gene phylogenetic analyses, respectively.

Toxin analysis. Reagents for chemical analyses. All organic
solvents and water (HPLC grade) and glacial acetic acid (Labo-
ratory grade) were by Sigma Aldrich (Steinheim, Germany).
A palytoxin standard (100 μg ; lot LAM7122) from Wako
Chemicals GmbH (Neuss, Germany) was dissolved in metha-
nol/water (1:1, v/v) and used for quantitative analyses. It
should be noted that this standard was not certified and may
have contained some contaminants other than the palytoxin
and that the quali-quantitative composition of this standard
can vary between lots. The standard used here contained
83% of palytoxin itself, 5% of 42-hydroxypalytoxin, and 12%
of contaminant(s). A crude extract of Ligurian *O. cf. ovata*
(CBA-29, Giussani et al. 2015) containing a pool of OVTXs
was used as a reference sample for identification of OVTXs
in algal extracts.

Toxin extraction. Cell pellets of five *Ostreopsis* strains col-
lected along Lebanon coasts, namely L1002 (8.0×10^6 cells),
L1007 (1.0×10^7 cells), L1008 (3.0×10^6 cells), L1020
(4.8×10^6 cells), L1022 (1.0×10^6 cells) were extracted once
by adding 1–10 mL of methanol/water (1:1, v/v) to achieve a
concentration of around $1.0 \times 10^6 \text{ cells} \cdot \text{mL}^{-1}$ of extracting
solvent. The mixtures were sonicated for 10 min in pulse
mode, while cooling in ice bath, and centrifuged at $3,000 g$
for 1 min; the obtained supernatants were then decanted
and analyzed by LC-HRMS (5 μL injected).

*Liquid chromatography-high resolution multiple stage mass spec-
trometry.* MS experiments (positive ions) were carried out on a
Dionex Ultimate 3000 quaternary system coupled to a
hybrid linear ion trap LTQ Orbitrap XLTM Fourier Transform
MS (FTMS) equipped with an ESI ION MAXTM source
(Thermo-Fisher, San José, CA, USA). A Poroshell 120 EC-
C18, 2.7 μm , $2.1 \times 100 \text{ mm}$ column (Agilent, USA) main-
tained at room temperature was used. It was eluted at
 $0.2 \text{ mL} \cdot \text{min}^{-1}$ with water (eluent A) and 95% acetonitrile/
water (eluent B), both containing 30 mM acetic acid. A slow
gradient elution was used: 28%–29% B over 5 min; 29%–30%
B over 10 min; 30%–100% B over 1 min, and held for 5 min
(Ciminiello et al. 2015).

HR full scan MS experiments (positive ions) were acquired
in the range m/z 800–1400 at a RP of 60,000 (FWHM at m/z
400). The following source settings were used: a spray voltage
of 4.8 kV, a capillary temperature of 290°C , a capillary voltage
of 17 V, a sheath gas and an auxiliary gas flow of 32 and 4
(arbitrary units). The tube lens voltage was set at 145 V. HR
collision induced dissociation MS² experiments were acquired
at a RP = 60,000 using a collision energy = 35%, isolation
width = 3.0 Da, activation Q = 0.250, and activation
time = 30 ms. The most intense peak of the $[\text{M}+\text{H}+\text{Ca}]^{3+}$
ion cluster of OVTX-a (m/z 896.1) and OVTX-d/-e (m/z 901.4)
were used as precursors in HRMS² experiments. Calculation
of elemental formulae was performed using the mono-isotopic
peak of each ion cluster using Xcalibur software v. 2.0.7
with a mass tolerance constrain of 5 ppm. The isotopic pat-
tern of each ion cluster was taken into account in assigning
molecular formulae. Extracted ion chromatograms of the
detected OVTXs were obtained by selecting the $[\text{M}+\text{H}+\text{Ca}]^{3+}$
ion clusters, using a mass tolerance of 5 ppm and employed

TABLE 1. List of *Ostreopsis* spp. isolates, sampling locations, isolator, ITS - 5.8S, and LSU gene sequence accession numbers from GenBank and EMBL.

Species	Strain ID	Geographical origin and collecting period	Isolator	Accession no. ITS-5.8S	Accession no. LSU
<i>O. cf. ovata</i>	CBA166	Trieste, Italy, Adriatic Sea, Mediterranean, 2009	Penna A.	JX065557	
<i>O. cf. ovata</i>	CBA1823	Taormina, Italy, Ionian Sea, Mediterranean, 2010	Battocchi C.	JX065555	
<i>O. cf. ovata</i>	CBA1597	Marina di Pisa, Italy, Tyrrhenian Sea, Mediterranean, 2010	Casabianca S.	JX065554	
<i>O. cf. ovata</i>	CBA1502	Alghero, Italy, Tyrrhenian Sea, Mediterranean, 2010	Capellacci S.	JX065553	JX065562
<i>O. cf. ovata</i>	CBA1553	Villefranche, Ligurian Sea, Mediterranean, France, 2010	Battocchi C.	JX065556	JX065565
<i>O. cf. ovata</i>	CBA N	Tyrrhenian, Mediterranean, Italy, 2007	Capellacci S.	FM244631	FM946085
<i>O. cf. ovata</i>	VGO 820	Catalan, Mediterranean, 2005	Fraga S.	FM244634	FM994892
<i>O. cf. ovata</i>	VGO 822	Catalan, Mediterranean, 2005	Fraga S.		FM994893
<i>O. cf. ovata</i>	VGO 884	Catalan, Mediterranean, 2005	Fraga S.		FM994931
<i>O. cf. ovata</i>	VGO960	Llavaneres, Spain, Catalan Sea, Mediterranean, 2008	Fraga S.		JX065567
<i>O. cf. ovata</i>	VGOOS20BR	Rio de Janeiro, Brazil, W Atlantic Ocean, 2000	Fraga S.		FM997919
<i>O. cf. ovata</i>	VGO1001	Famara, Canary Island, Spain, E Atlantic Ocean, 2008	Rodriguez F.	JX065551	
<i>O. cf. ovata</i>	VGO1056	Belize, Caribbean Sea, N Atlantic Ocean, 2009	Holland C.	JX065586	JX065588
<i>O. cf. ovata</i>	KC34	Aegean, Mediterranean, 2004	Aligizaki K.	FM242104	FM946092
<i>O. cf. ovata</i>	KC71	Aegean, Mediterranean, 2004	Aligizaki K.	FM244735	FM946099
<i>O. cf. ovata</i>	OS18BR	West Atlantic, Brazil, 2000	Fraga S.	FM244670	FM997918
<i>O. cf. ovata</i>	CBA4	East Pacific, Indonesia, 2007	Penna A.		FM997921
<i>O. cf. ovata</i>	CBA9	East Pacific, Indonesia, 2007	Penna A.	FM244726	
<i>O. cf. ovata</i>	OvPD06	Indian, Malaysia, 1997	Pin L.C.	AF218455	
<i>O. cf. ovata</i>	OvSA04	Indian, Malaysia, 1997	Pin L.C.	AF218461	
<i>O. cf. ovata</i>	PR-03	Indian, Malaysia, 1997	Pin L.C.	AF076218	
<i>O. cf. ovata</i>	OvSA06	Indian, Malaysia, 1997	Pin L.C.	AF218463	
<i>O. cf. ovata</i>	CAWD174	Rarotonga, Cook Island, 2009	Strickland R. Sellwood A.	AB674904	
<i>O. cf. ovata</i>	KabO13	Okinawa, Ishigaki, Kabira, Japan 2010	Suda S.		AB605817
<i>O. cf. ovata</i>	IshiOst50	Okinawa, Ishigaki, Shiraho, Japan, 2009	Shah M.R.		AB605824
<i>O. cf. ovata</i>	QB04	Quang Binh, Vietnam, South China Sea, Pacific, 2009	Nguyen N.L.		JX065571
<i>O. cf. ovata</i>	QB06	Quang Binh, Vietnam, South China Sea, Pacific, 2009	Nguyen N.L.		KC900891
<i>O. cf. ovata</i>	QB03	Quang Binh, Vietnam, South China Sea, Pacific, 2009	Nguyen N.L.		KC900890
<i>O. cf. ovata</i>	LCH001	Thua Thien-Hue, Vietnam South China Sea, Pacific, 2009	Nguyen N.L.		JX065569
<i>O. cf. siamensis</i>	IO-9601	Sines, Portugal, E Atlantic, 2008	Veloso V.	JX065587	
<i>O. cf. siamensis</i>	OS-2V	Alboran, Mediterranean, 1999	Fraga S.	AJ491313	
<i>O. cf. siamensis</i>	OS-5V	Alboran, Mediterranean, 1999	Fraga S.		FN256430
<i>O. cf. siamensis</i>	CSIC-D7	Catalan, Mediterranean, 2000	Garcés E.	AJ491334	FN256431
<i>O. cf. siamensis</i>	CNR-B4	Tyrrhenian Sea, Mediterranean, 2000	Giacobbe M.G.	AJ301643	
<i>O. cf. siamensis</i>	CAWD96	Kerikeri, New Zealand, 1999	North Health Services	AB674915	
<i>O. cf. siamensis</i>	Dn17EHU	Biscay, Spain, 2007–2009	Laza A.		HQ414225
<i>O. cf. siamensis</i>	Dn 20EHU	Biscay, Spain, 2007–2009	Laza A.		HQ414224
<i>O. cf. siamensis</i>	Dn18EHU	Biscay, Spain, 2007–2009	Laza A.		HQ414222
<i>O. cf. siamensis</i>	Dn171EHU	Saint Jean de Luz, France, 2010	David H.	JX987690	
<i>O. cf. labens</i>	VGO897	Indian, Malaysia, 1997	Mohammad N.	FM244728	
<i>O. cf. lenticularis</i>	NT011	Ninh Thuan, Vietnam, South China Sea, 2009	Nguyen N.L.	JX065584	
<i>O. cf. lenticularis</i>	NT013	Ninh Thuan, Vietnam, South China Sea, 2009	Nguyen N.L.		JX065570
<i>O. cf. lenticularis</i>	OLPR01	Indian, Malaysia, 1997	Pin L.C.	AF218465	AF244941
<i>Ostreopsis</i> sp.	TB34OS	Khao Lak, Phang-Nga, Thailand, 2015	Tawong W.	AB841214	
<i>Ostreopsis</i> sp.	TB35OS	Khao Lak, Phang-Nga, Thailand, 2015	Tawong W.	AB841215	
<i>Ostreopsis</i> sp.	TB33OS	Khao Lak, Phang-Nga, Thailand, 2015	Tawong W.	AB841213	
<i>Ostreopsis</i> sp.	KC84	Cyprus, Aegean Sea, Mediterranean, 2008	Aligizaki K.	JX065549	JX065558
<i>Ostreopsis</i> sp.	KC86	Crete, Greece, Aegean Sea, Mediterranean, 2009	Aligizaki K.	JX065550	JX065559
<i>Ostreopsis</i> sp.	CBA0203	Honolulu, Hawaii, N Pacific Ocean, USA, 2010	Capellacci S.	JX065552	JX065561
<i>Ostreopsis</i> sp.	VGO881	Canary Island, East Atlantic, 2005	Fraga S.	FM244637	FM994895
<i>Ostreopsis</i> sp.	Dn83EHU	Crete, Greece, 2010	David H.	JX987673	
<i>Ostreopsis</i> sp.	Dn110EHU	Puerto Rico, North America 2011	David H.	JX987680	
<i>Ostreopsis</i> sp.	TF29OS	Koh Wai, Trat, Thailand, 2011	Tomohiro N.	AB841255	
<i>Ostreopsis</i> sp.	TF25OS	Koh Wai, Trat, Thailand, 2011	Tomohiro N.	AB841254	
<i>O. fattorusoi</i>	CBA C1005	Cyprus, Aegean Sea, Mediterranean, 2013	Capellacci S.	LT220222	
<i>O. fattorusoi</i>	CBA C1012	Cyprus, Aegean Sea, Mediterranean, 2013	Capellacci S.	LN875554	
<i>O. fattorusoi</i>	CBA C1019	Cyprus, Aegean Sea, Mediterranean, 2013	Capellacci S.	LN875552	LT555465
<i>O. fattorusoi</i>	CBA C1020	Cyprus, Aegean Sea, Mediterranean, 2013	Capellacci S.	LN875556	LT555466

(continued)

1 TABLE 1. (continued)

Species	Strain ID	Geographical origin and collecting period	Isolator	Accession no. ITS-5.8S	Accession no. LSU
<i>O. fattorussoi</i>	CBA C1035	Cyprus, Aegean Sea, Mediterranean, 2013	Capellacci S.	LN875553	
<i>O. fattorussoi</i>	CBA C1036	Cyprus, Aegean Sea, Mediterranean, 2013	Capellacci S.	LN875557	
<i>O. fattorussoi</i>	CBA L1000	Batroun, Lebanon, Mediterranean, 2014	Capellacci S.	LT220223	
<i>O. fattorussoi</i>	CBA L1020	Batroun, Lebanon, Mediterranean, 2014	Capellacci S.	LT220224	LT555467
<i>O. fattorussoi</i>	CBA L1007	Batroun, Lebanon, Mediterranean, 2014	Capellacci S.		LT555468
<i>O. fattorussoi</i>	CBA L1008	Batroun, Lebanon, Mediterranean, 2014	Capellacci S.		LT555469
<i>O. fattorussoi</i>	CBA L1022	Batroun, Lebanon, Mediterranean, 2014	Capellacci S.		LT555470
<i>Ostreopsis</i> sp.	UrGt12	Okinawa, Urasoe, off camp Kinser, Japan, 2009	Suda S.		AB605813
<i>Ostreopsis</i> sp.	UrGm6	Okinawa, Urasoe, off camp Kinser, Japan, 2009	Suda S.		AB605815
<i>Ostreopsis</i> sp.	IkeOst2	Ikejima, Uruma, Okinawa, Japan 2008	Suda S.		AB605814
<i>Ostreopsis</i> sp.	OA21-C10	Okinawajima Island, Japan	Nakashima A.		AB605828

18 in quantitative analyses. Due to availability of the only palytoxin standard, quantitative determination of OVTX-a, -d, and -e in the extracts was carried out by using a calibration curve (triplicate injection) of palytoxin standard at seven concentrations (1,000, 500, 250, 125, 62.5, 31.2, and 15.6 ng · mL⁻¹). OVTX molar responses were assumed to be similar to that of PLTX. Calibration curve equation was $y = 2,455.6x - 19,184$ and its linearity was expressed by $R^2 = 0.9976$. The limit of detection for palytoxin in pure solvent was 13 ng · mL⁻¹ after correction for the 83% purity of the standard.

29 RESULTS

31 ***Ostreopsis fattorussoi* Accoroni, Romagnoli et Totti**
32 **sp. nov.**

33 **Diagnosis.** Cells are ovate in shape and ventrally
34 pointed with a DV of 42.5–72.5 µm, AP of 20–
35 32.5 µm and transdiameter 26.3–50 µm. The thecal
36 plate formula is Po, 3', 7", 6c, 7s, 5"', 2'''''. Thecal
37 plates are smooth with evenly distributed same-sized
38 round pores. The apex is strongly eccentric, located
39 on the left dorsal side of the epitheca. The apical
40 pore plate Po is 10–12.5 µm long and slightly
41 curved. Plate 1' is heptagonal, oblique, and is almost
42 entirely in the left-half of the epitheca. Plate 3' is
43 hexagonal, almost entirely in the left-half of the
44 epitheca. The pentagonal 6" has the 6"/5" suture
45 length almost twice as long as the 6"/7" suture
46 length. The narrow sulcal groove runs obliquely
47 from the left side of the ventral area into the
48 hypotheca. Cells are photosynthetic. The nucleus
49 has a slightly elongated (subspherical) shape posi-
50 tioned obliquely and occupies the dorsal part of the
51 cell. The species is toxic producing ovatoxins.

52 **Holotype.** SEM stub n. 3/16-UNIVPM deposited at the
53 Botanical Museum of the Università Politecnica delle
54 Marche, Ancona Italy, in the Herbarium Anconitanum
55 (ANC). Figure 5A represents the holotype.

56 **Isotype.** Preserved sample, deposited at the Univer-
57 sità Politecnica delle Marche, Ancona Italy, in the
58 Herbarium Anconitanum (ANC).

59 Preserved DNA of clonal strain CBA-L1020, bar-
60 coded in ENA-EMBL (EMBL ID: LT220224), held

at the Dipartimento di Scienze Biomolecolari, Università di Urbino, Italy.

Type Locality. Batroun, Lebanon (34°15' 5.40" N, 35°39' 24.78" E, Fig. 1).

Habitat. Benthic, often epiphytic on seaweeds or living on other substrata; it was shown that it could also be resuspended into the water column.

Etymology. The specific epithet honors our dear colleague Prof. Ernesto Fattorusso from the University of Napoli Federico II, who significantly contributed to the study of algal biotoxin structures and elucidation of novel organic metabolites produced by marine algae.

Distribution: Eastern Mediterranean (i.e., Cyprus, Lebanon coasts). The same genotype is known also in Crete (David et al. 2013, Penna et al. 2014), Canary Islands, Spain (Penna et al. 2010) and Puerto Rico, USA (David et al. 2013).

Morphology. Cells are ovate and ventrally slender with average DV 60.1 ± 5.6 (42.5–72.5) µm, AP 25.7 ± 3 (20–32.5) µm, and W 39.8 ± 5.1 (26.3–50) µm. The DV:AP ratio is 2.35 ± 0.22 , while DV:W is 1.52 ± 0.14 .

The thecal plate formula is Po, 3', 7", 6c, 7s, 5"', 2'''' (Figs 2 and 3). Thecal plates are smooth with evenly distributed round pores visible using LM with Calcofluor-White M2R staining (Fig. 4A). Small perforations are located inside the pores (Fig. 5E). They are scattered on the epi- and hypothecal plates and lined up along the border of the pre- and postcingular plates close to the cingular groove (Fig. 5, A and B) and the borders of the two cingular lists (Fig. 5D). Only one size class pore is visible ranging from 0.26 to 0.53 µm (0.38 ± 0.08 µm) with 11–15 pores per 100 µm². Cells produce extracellular mucilage and a complex network of filaments is extruded through the thecal pores (Fig. 6D).

Both epitheca and hypotheca are equal in size. The apex is strongly eccentric, located on the left dorsal side of the epitheca. The apical pore plate Po is 11.67 ± 1.44 µm long, slight curved and contacts the three apical plates. Plate 1' is heptagonal

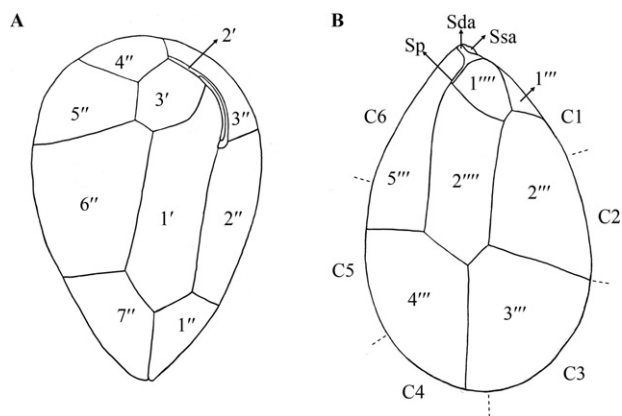


FIG. 2. *Ostreopsis fattorusoi*. Schematic drawings with plate tabulation of (A) epitheca, (B) hypotheca and cingulum. Sda, right-anterior sulcal; Ssa, left anterior sulcal plate; Sp, posterior sulcal plate.

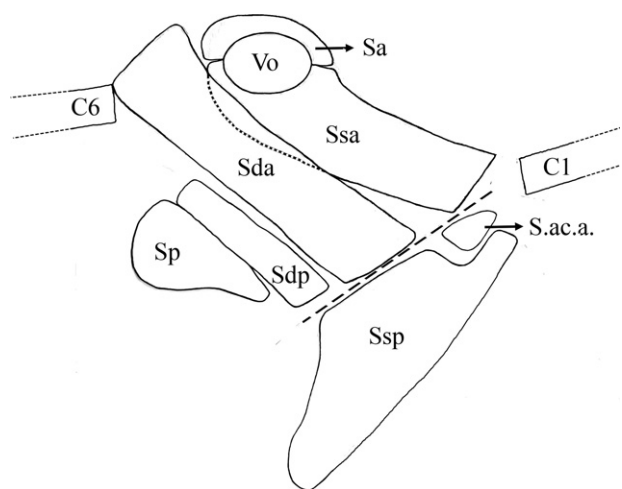


FIG. 3. Interpretation drawing of the sulcus of *Ostreopsis fattorusoi*. Sa, anterior sulcal plate; Ssa, left anterior sulcal plate; Sda, right-anterior sulcal plate; Sdp, right-posterior sulcal plate; Sp, posterior sulcal plate; Ssp, left posterior sulcal plate; S.ac.a., accessory anterior sulcal plate; dotted line indicates the position of the bottom of the sulcus (Sa, Ssa, Sda, Sdp, and Sp are in the upper side of the sulcus groove and Ssp and S.ac.a. are in the inferior side of the sulcus); Vo, ventral opening.

and almost entirely lies in the left-half of the epitheca and is not parallel to the dorsoventral axis, but its dorsal part is shifted on the left and dorsally pointed. Plate 1' touches plates 2', 3', 1'', 2'', 6'', and 7''. Plate 2' is narrow and almost twice the size of Po, separating the 3' and 3'' plates. Plate 3' is hexagonal, almost entirely located in the left-half of the epitheca, and it is dorsally displaced.

Among the seven irregularly quadrangular (with the only exception of the plate 6'') precingular plates 1'' and 4'' are the smallest. Because of the left and dorsal displacement of 3', plate 5'' is transversally elongated and 3'' appears as narrow and

dorsally elongated as plate 2'' (Figs. 4, A and C; 5A). The characteristic shape of the pentagonal 6'' is due to the oblique orientation of the 1' and the 6''/5'' suture length is almost twice as long as 6''/7'' suture length, resulting in an oblique 6''/1' suture; moreover, its length:width ratio is 1.06 ± 0.11 (0.94–1.2) and the 3'/6'' suture is dorsally shifted. The first and the last precingular plates (i.e., 1'' and 7'', respectively) are extended and elongated, tapering toward the sulcal area. Plate 2'' is narrow and the 4'' has a similar size of 3'.

The cingulum is descending and displaced one time its width and consists of six plates, almost of the same length.

The narrow sulcal groove runs obliquely from the left side of the ventral area into the hypotheca. The ventral side of the 1'''' plate forms a "wing" that covers almost all the sulcal area of the hypotheca (Fig. 4, D–F) leading well identifiable only 5 plates in intact cells (Fig. 6A): the anterior sulcal plate (Sa), the left anterior sulcal plate (Ssa), the right-anterior sulcal plate (Sda), the right-posterior sulcal plate (Sdp), and the posterior sulcal plate (Sp). In broken cells, a further two plates are identifiable on the inner left side of the sulcus: the left posterior sulcal plate (Ssp) and the accessory anterior sulcal plate (S.ac.a.) (Fig. 6, B and C).

In the upper part of the ventral area, a conspicuous tube-like structure, the ventral tube (Vt), ends with an opening (ventral opening; Figs. 4D and 6, A and B). The upper half of the Vt is surrounded by the small Sa and the lower half by the elongated Ssa. The Sa is small and touches the ventral part of the 1'' and 7'' plates. The Ssa plate is wide and extends from the lower side of the Sa and Vt to the first cingular plate (C1) and the S.ac.a. plate. The left (i.e., the anterior) margin of the Ssa plate touches the 1'' plate, while the right (i.e., the posterior) margin is in contact with the anterior, sigmoid edge of the Sda plate.

The Sda plate is the most elongated of all the sulcal plates. Its anterior part is curved toward the epitheca and contacts, from right to left, the sixth cingular (C6), the 7'' and the Sa plates. It surrounds the right (i.e., the posterior) margin of plate Ssa along its whole side. The left portion of the Sda plate is hidden by the 1'''' and contacts the Ssp plate in the bottom of the sulcal groove. At its posterior part, Sda contacts the ventral end of the 5'' and the narrow Sdp.

In the end of the sulcal groove, the right-anterior part of the irregularly triangular Sp touches the ventral end of the 5'' plate, and its right-posterior part adjoins to a small portion of the ventral end of the 2'''' plate (Fig. 4E). The upper part of the Sp connects with the Sdp and in its posterior part to the Ssp.

The other side of the sulcal groove (and therefore completely covered by the 1'''' plate) consists of the almost quadrangular S.ac.a. plate for the small

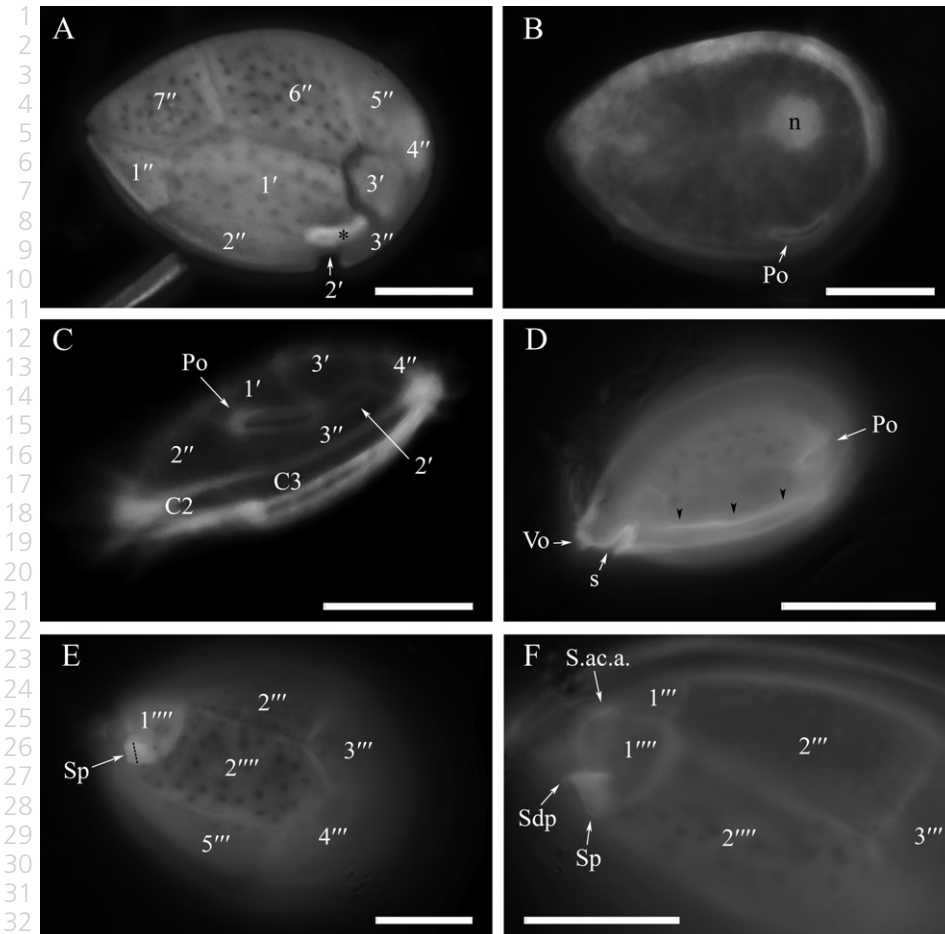


FIG. 4. *Ostreopsis fattorussoi*, light microscopy micrographs. Epifluorescence observations after Calcofluor-White of cells from natural samples. (A) Epitheca (* = apical pore plate Po). (B) Apical view of a cell stained with SYBR Green highlighting the nucleus (apical pore plate Po is visible). (C) Left lateral view showing the contact of plate 2' with 4''. (D) Merging of several photograms taken at different foci of the left lateral side of a cell showing the depth of the sulcus (s) and the ventral opening (Vo); arrowheads indicate the cingulum border in the epitheca. (E, F) Hypotheca; (E) focus on the posterior sulcal plate (Sp): although the Sp is almost entirely covered by the plate 1'''' (dotted line indicates the position of the 1'''' border on the Sp plate), the focus allows observing the entire plate and its small contact with plate 2''''; (F) focus on the plates Sdp and S.ac.a. under the 1'''' . Scale bars = 20 μ m.

upper part (Fig. 6C) and the elongated Ssp makes up rest of the groove.

Among the five postingular plates, the triangular 1''' plate is the smallest of the series. The 2''' plate is wide and quadrangular. The quadrangular 3''' and 4''' plates occupy most of the dorsal part of the hypotheca, while the 5''' plate is oblong and quadrangular, although the ventral side is very short. There are two antapical plates which are both pentagonal. The 1'''' plate is much smaller than the 2'''' plate which occupies the center of the hypotheca (Figs. 4, E and F; 5B).

There are numerous elongated chloroplasts located within the cell periphery. The nucleus, has a slightly elongated (often subspherical) shape (13.6 \pm 2.0 μ m long, 8.8 \pm 1.7 μ m wide) positioned obliquely in the dorsal part (from the right to the center) of the cell (Fig. 4B).

Phylogenetic analyses of Ostreopsis ITS-5.8S and LSU ribosomal genes. The final alignments of *Ostreopsis* spp. ribosomal gene sequences, as ITS-5.8S and LSU with *Coolia monotis* VGO783 and VGO786 as out-groups, respectively, were as follows: ITS-5.8S was 419 bp in length (A = 27%, T = 34.8%, C = 18.2%, G = 20%) with 116 polymorphic sites, of which 93 parsimony informative, and a transition/

transversion ratio of 1.7; LSU was 701 bp in length (A = 28.5%, T = 32.9%, C = 16.9%, G = 21.7%) with 343 polymorphic sites, of which 284 parsimony sites, and a transition/transversion ratio of 1.4.

Based on single ITS-5.8S and LSU rDNA sequences, only minor differences between the NJ, MP, ML and Bayesian inference analyses were found; therefore, only the ML phylogenetic trees are presented (Figs. 7 and 8). The ITS-5.8S rDNA phylogeny, based on 46 isolates of *Ostreopsis* spp., identified three major clades within the genus *Ostreopsis*: the first comprising *Ostreopsis* sp. CBA0203 from Hawaii, and strains identified as *O. cf. lenticularis*, *O. cf. labens* and *Ostreopsis* sp. 6 (Tawong et al. 2014) from Pacific Ocean; the second clade comprised the *O. cf. siamensis*, and *Ostreopsis* sp. (now identified as *O. fattorussoi*) from eastern Mediterranean Sea, Greece (KC84, KC86, Penna et al. 2014 and Dn83EHU, David et al. 2010), Lebanon and Cyprus (this study), with *Ostreopsis* sp. VGO881 (Canary Islands) and *Ostreopsis* sp. Dn110EHU (Porto Rico) from Atlantic Ocean. Finally, the third grouping included *O. cf. ovata* complex from Atlantic, Mediterranean, and Pacific. All these clusters were supported by high bootstrap and posterior probability values.

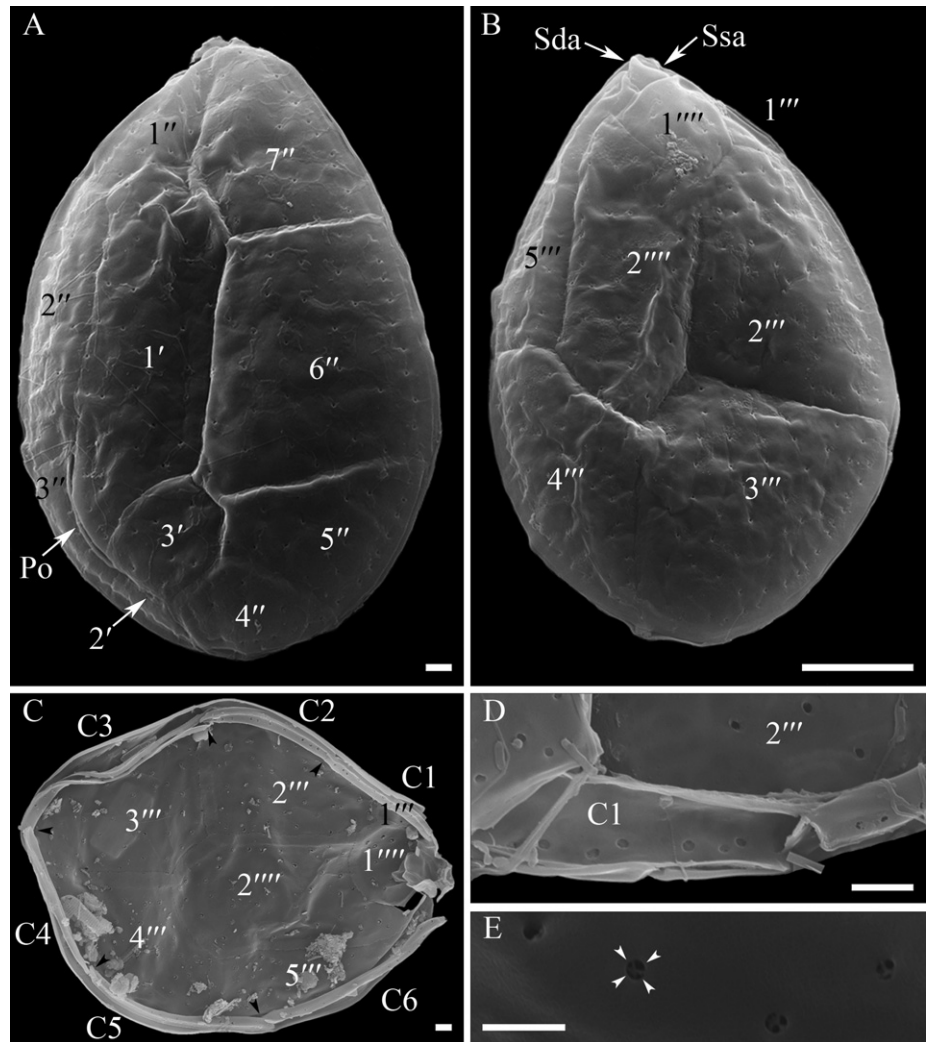


FIG. 5. *Ostreopsis fattorussoi*, SEM micrographs. (A) Epitheca. (B) Hypotheca. (C) Internal view of the hypotheca showing the cingular plates with distinctive borders (arrowheads) between two adjacent plates. (D, E) Magnification on the internal side of the hypotheca showing the thecal pores; (D) pores lined up along both the borders of the two cingular lists; (E) small perforations inside thecal pores. Po, apical pore plate; Sda, right-anterior sulcal; Ssa, left anterior sulcal plate. Scale bars = 2 μm (A, C, D, and E); 10 μm (B).

The LSU rDNA phylogeny that was obtained from 40 isolates of *Ostreopsis* spp. showed some differences in tree topology compared with ITS-5.8S rDNA phylogenetic analysis. The first splitting clade from outgroup *Coolia* included two sub-clades of *O. cf. lenticularis* and *Ostreopsis* sp. along with *Ostreopsis* sp. 5 and *Ostreopsis* sp. CBA0203; all these isolates derived from Indian and Pacific Ocean. The second clade grouped the *Ostreopsis* sp. (now identified as *O. fattorussoi*) from eastern Mediterranean Sea (Lebanon, Greece and Cyprus) and Atlantic VGO881 isolate. The third clade comprised all *O. cf. ovata* isolates collected from many sites worldwide and *O. cf. siamensis*. All these lineages were strongly supported by high bootstrap and posterior probability values.

The difference of base pair between *O. fattorussoi* and other *Ostreopsis* species ranged from 200 to 231 bp, and from 99 to 82 bp based on LSU and ITS-5.8S rDNA analysis of net nucleotide average difference, respectively.

Temporal trend and relationships with environmental parameters. *Ostreopsis* cells were detected at the

Batroun site throughout the year with two blooming periods, the first observed between the end of May and the beginning of July and the second in August (Fig. 9B). Maximum abundances were detected on 2 July 2015 ($28 \times 10^3 \text{ cells} \cdot \text{g}^{-1} \text{ fw}$) and on 22 June 2015 ($840 \text{ cells} \cdot \text{L}^{-1}$) on benthic substrata and in the water column, respectively.

The correlation between *Ostreopsis* abundances on benthic substrata and those in water column was positive and significant ($n = 9$; $r = 0.79$; $P < 0.05$).

Surface temperature ranged from 18°C to 31.5°C with maximum temperatures of 29.5°C to 31.5°C occurring from the end of July to early October and minimum values of around 18°C in the first months of the year. The maximum values of *Ostreopsis* abundances were recorded when water temperature ranged from 27°C to 29.7°C (Fig. 9B). Throughout the year, the salinity ranged from 38.14 to 39.43. Correlation analyses among *Ostreopsis* abundances, growth rate, temperature, and salinity revealed no significant relationships.

No obvious trends were determined for of NO_2 , NO_3 and PO_4 (Fig. 9A). Only NO_3 showed high

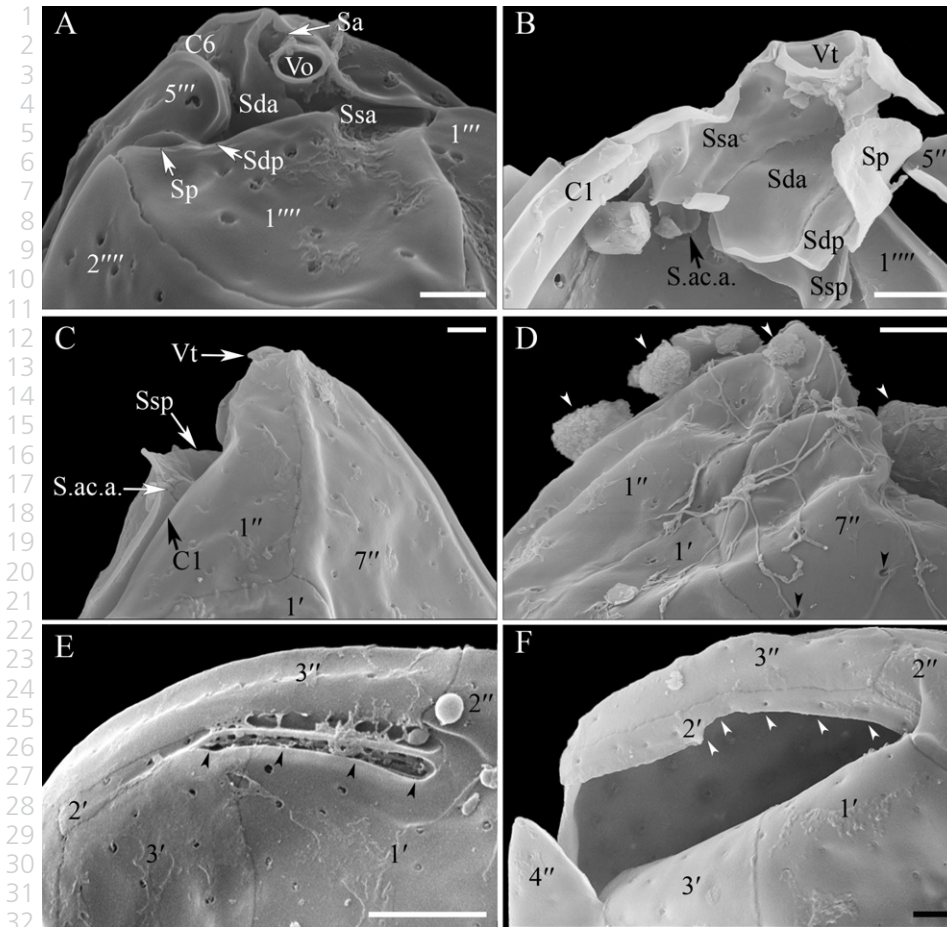


FIG. 6. *Ostreopsis fattorussoi*, SEM micrographs. (A) Ventral area in an intact cell. (B) Internal view of the hypotheca and the sulcus in a broken cell showing all the sulcal plates (with the exception of Sa): Ssa, Sda, Sdp, and Sp are in the upper side of the sulcus groove and partially cover Ssp and S.ac.a. which are in the inferior side of the sulcus; Sp is unnaturally bended leading show the space between the 1''' and 5''' plates. (C) Left lateral view of the ventral area partially showing the inferior side of the sulcus. (D) Apical ventral view of a cell showing a complex network of filaments released by the thecal pores (black arrowheads) and extracellular mucilage (white arrowheads). (E, F) Magnification on the apical dorsal part showing the apical pore plate Po; (E) intact Po (black arrowheads) and the plate 2'; (F) suture between the plate 2' and the Po which is missing (white arrowheads). Scale bars = 2 μm (A, B, C, D, and F); 5 μm (E).

35 values ($>1.3 \mu\text{mol} \cdot \text{L}^{-1}$) in January and February
 36 compared with the rest of the year, when values ran-
 37 ged from 0.156 to 0.626 $\mu\text{mol} \cdot \text{L}^{-1}$. NO_2 concentra-
 38 tions were markedly lower than those of nitrates,
 39 ranging from 0.015 to 0.250 $\mu\text{mol} \cdot \text{L}^{-1}$. No signifi-
 40 cant relationships were found between *Ostreopsis*
 41 abundances (or growth rate) and both NO_2 and
 42 NO_3 . PO_4 concentrations ranged from 0.015 to
 43 0.433 $\mu\text{mol} \cdot \text{L}^{-1}$ and rarely exceeded 0.150 $\mu\text{mol} \cdot$
 44 L^{-1} throughout the year. The two maximum values
 45 of PO_4^{3-} , that is, 0.433 and 0.175 $\mu\text{mol} \cdot \text{L}^{-1}$, were
 46 recorded in February and June, respectively.
 47 Although no correlation between *Ostreopsis* abun-
 48 dances and PO_4 concentrations was detected, a posi-
 49 tive and significant correlation was found between
 50 *Ostreopsis* growth rates and PO_4 concentrations
 51 ($n = 9$; $r = 0.87$; $P < 0.01$).

52 **Toxicity.** Crude extracts of five strains of *O. fat-*
 53 *torussoi* collected along the Lebanese coast (i.e.,
 54 L1002, L1007, L1008, L1020, and L1022) were ana-
 55 lyzed by LC-HRMSⁿ ($n = 1, 2$) to characterize their
 56 toxin profiles and measure their toxin content. The
 57 analyses were carried out with a palytoxin standard
 58 and a Ligurian *O. cf. ovata* extract containing
 59 OVTX-a, -d and -e and isobaric palytoxin (Giussani
 60 et al. 2015). The chromatographic conditions

allowed the separation of all of the analogs con-
 tained in the extracts.

Toxin extracts from the five Lebanese strain of *O. fattorussoi* revealed three strains to be toxic; L1007, L1020, and L1022 all contained OVTX-a, -d, and -e. Their identity was ascertained based on comparison of their retention times and associated full MS spectra (Fig. 10) with those of OVTX-a, -d, -e, contained in the reference extract. Further confirmation for the identity of OVTX-a and of the structural isomers OVTX-d and -e was provided by their LC-HRMS² spectra.

Extracts L1002 and L1008 did not contain any palytoxin congener. Considering the extraction volume, the presence of toxins in pellet (1×10^6 cells), could be excluded at levels $\leq 15 \text{ fg} \cdot \text{cell}^{-1}$.

The results of the quantitative analysis are shown in Table 2.

DISCUSSION

In the Mediterranean Sea, only two *Ostreopsis* species have been recorded until now, *O. cf. ovata* and *O. cf. siamensis* (Vila et al. 2001, Penna et al. 2005, 2010, Battocchi et al. 2010, Totti et al. 2010, Mangialajo et al. 2011, Perini et al. 2011, Mabrouk et al.

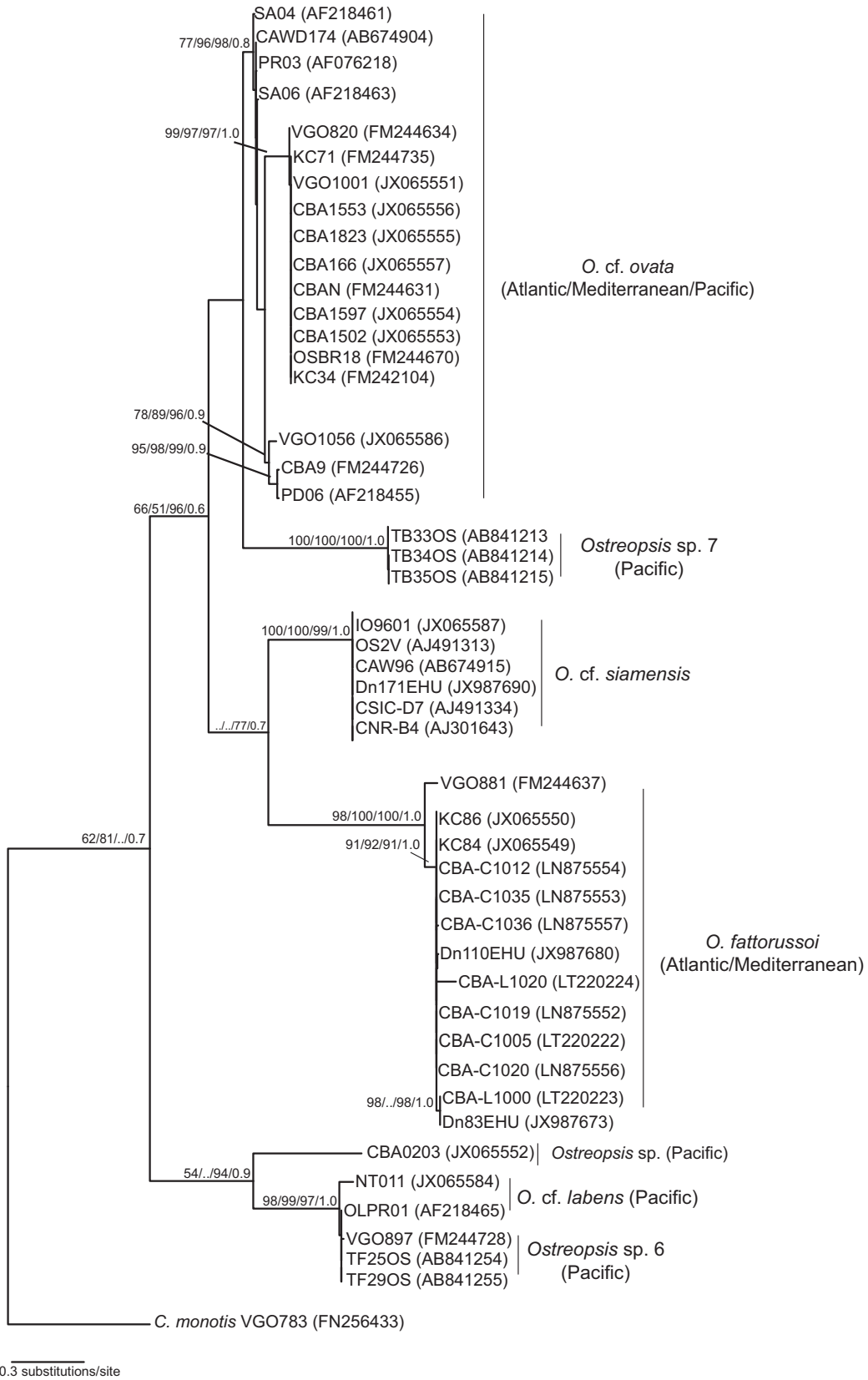


FIG. 7. Maximum likelihood phylogenetic tree of the genus *Ostreopsis* inferred from ITS-5.8S ribosomal gene sequences. The tree is rooted with *Coolia monotis* VGO783 as outgroup. Numbers on the major nodes represent from left to right NJ (1,000 pseudo-replicates), MP (1,000 pseudo-replicates), ML (1,000 pseudo-replicates) bootstrap and Bayesian posterior probability values. Only bootstrap values >50% are shown. Geographical origins of *Ostreopsis* isolates are indicated.

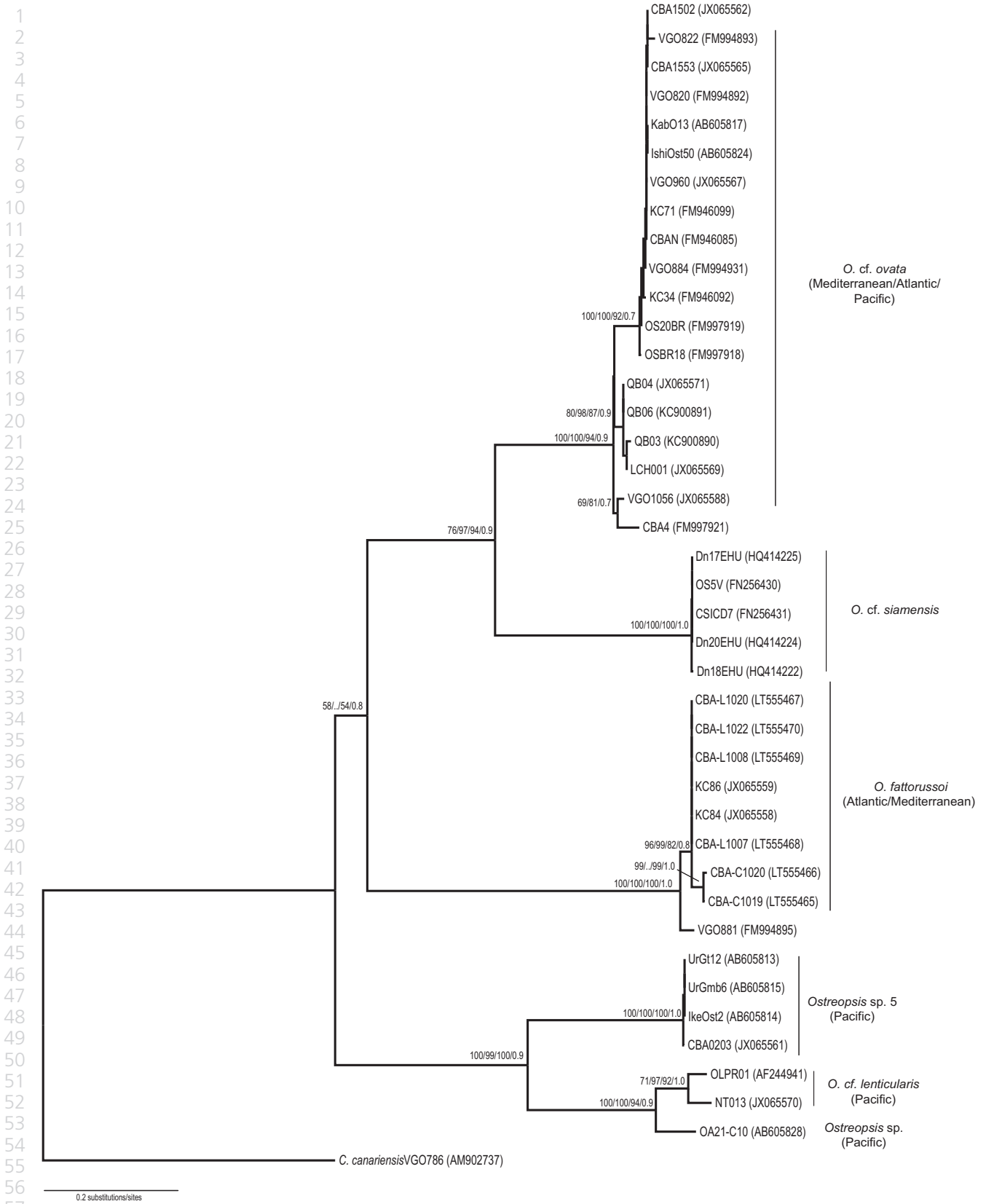


FIG. 8. Maximum likelihood phylogenetic tree of the genus *Ostreopsis* inferred from LSU ribosomal gene sequences. The tree is rooted with *Coolia monotis* VGO786 as outgroup. Numbers on the major nodes represent from left to right NJ (1,000 pseudo-replicates), MP (1,000 pseudo-replicates), ML (1,000 pseudo-replicates) bootstrap and Bayesian posterior probability values. Only bootstrap values >50% are shown. Geographical origins of *Ostreopsis* isolates are indicated.

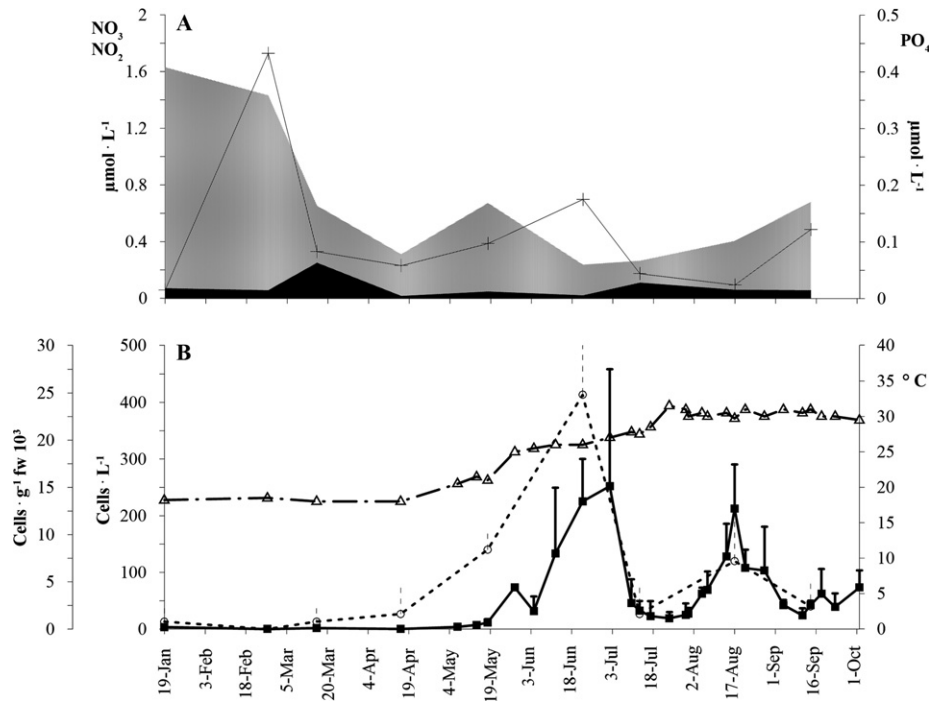


FIG. 9. Trend in nutrient concentration, temperature and *Ostreopsis fattorussoi* abundances both on benthic macroalgae and in water column in Batroun (Lebanon) during 2015. (A) Nutrient concentration ($\mu\text{mol} \cdot \text{L}^{-1}$): inorganic nitrogen with the detail of NO_3 and NO_2 (gray and black, respectively, left y-axis), and PO_4 (line, right y-axis). (B) *O. fattorussoi* abundances on seaweeds (■, 1st left y-axis) and in the water column (○, 2nd left y-axis) expressed in $\text{cells} \cdot \text{g}^{-1} \text{fw}$ and $\text{cells} \cdot \text{mL}^{-1}$, respectively. Temperature values expressed in $^{\circ}\text{C}$ (▲, right y-axis). Error bars indicate standard deviations.

2012, Abboud-Abi Saab et al. 2013, Accoroni and Totti 2016). Recently, new molecular phylogenetic analyses based on ribosomal DNA identified another clade (*Ostreopsis* sp.) distinct from *O. cf. ovata* and *O. cf. siamensis*, in the eastern Atlantic and Mediterranean coasts, particularly from islands of Cyprus and Crete (Penna et al. 2012, Tartaglione et al. 2015). In this study, we name and describe this new genotype as a new species of *Ostreopsis*, named *O. fattorussoi*, by analyzing samples from coasts of Lebanon and Cyprus (Mediterranean Sea).

In this study, the description of the thecal tabulation and the morphometrical analyses of this new species were performed on field samples only, as cultured specimens of *O. fattorussoi* frequently demonstrated modifications in shape, size and thecal pattern, as already reported in other *Ostreopsis* species (Norris et al. 1985, Laza-Martinez et al. 2011, Nascimento et al. 2012, Scalco et al. 2012, David et al. 2013). For example, a cultured Indonesian strain of *O. cf. ovata* (CBA-6) has been observed either to show (Parsons et al. 2012) or not (Penna et al. 2010) the contact between the $1'$ and $5''$ plates, which is a defining plate pattern character of *O. heptagona*. The numerous strains of *O. fattorussoi* were used to characterize the toxic profile and to perform the molecular sequencing of this new species.

The plate tabulation of *Ostreopsis* has been frequently reassessed over the years from its first

descriptions (Table 3). The first interpretations of the thecal plates were given by Schmidt (1901) and later by Fukuyo (1981), who included a partial plate formula of Po, $3'$, $7''$, $4'''$ (+ accessory small plates), 1 antapical plate and Po, $3'$, $7''$, $5'''$, $1''''$, respectively. This plate pattern interpretation based on Kofoidian plate tabulation was adopted by Norris et al. (1985) and Faust et al. (1996) who, however, labeled the large hypothetical plate at the antapex (i.e., $1''''$ in Fukuyo (1981)) as a posterior intercalary plate (1p). Over the years, several other authors followed this plate pattern interpretation, although often with a little variation (Penna et al. 2005, Sato et al. 2011, Kang et al. 2013, Hoppenrath et al. 2014).

On the contrary, Besada et al. (1982) did not follow the plate pattern suggested by Fukuyo (1981) but reinterpreted the apical plate pattern, providing for the first time a complete plate formula (Po, $4'$, $6''$, $6c$, $8s$, $5'''$, $2''''$) which was closer to that of gonyaulacoid dinoflagellates. In this view, the epithelial tabulation was strongly rearranged as the plate considered as $1''$ (precingular) in Fukuyo (1981) and Faust et al. (1996) was considered homologous to the first apical plate of the Gonyaulacales and therefore was named $1'$. As a consequence, the plate tabulation included four apical and six precingular plates. This interpretation has been re-adopted by Escalera et al. (2014) for *Ostreopsis cf. ovata* and was applied to *Gambierdiscus*

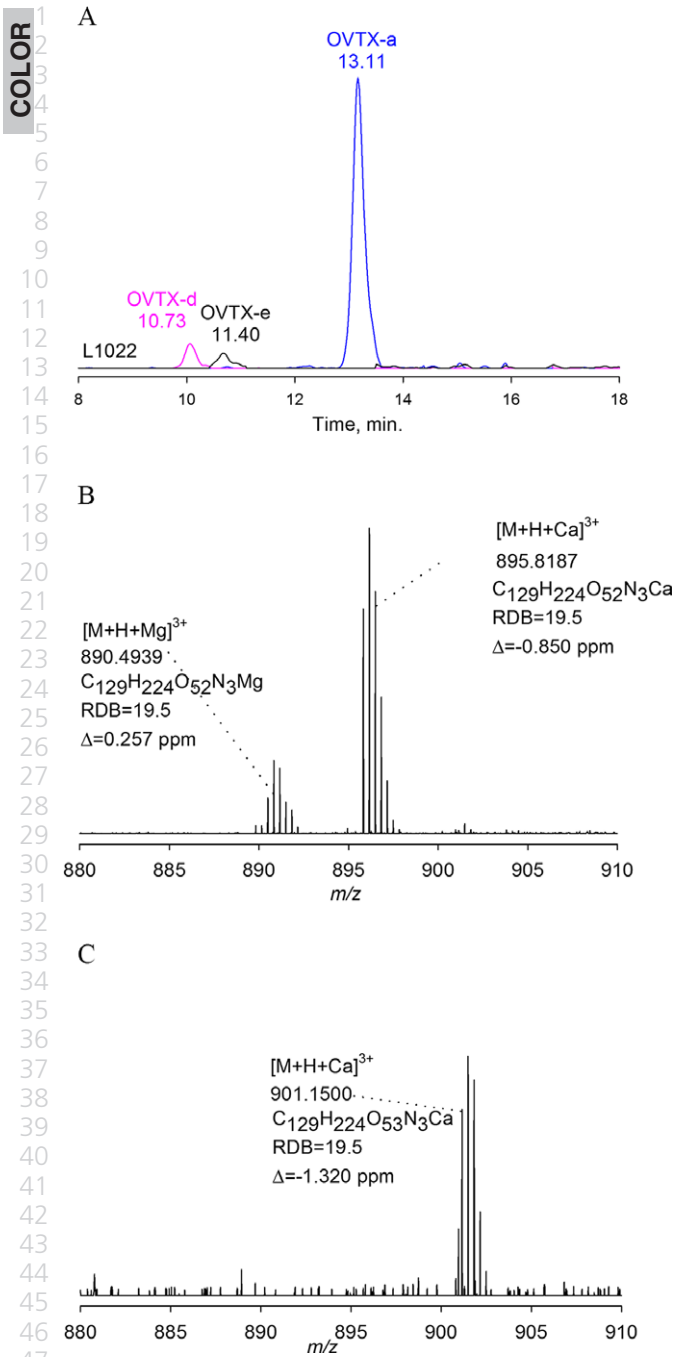


FIG. 10. LC-HRMS analysis of *Ostreopsis fattorussoi* L1022 strain, including (A) extracted ion chromatogram (XIC) of $[M+H+Ca]^{3+}$ ions of ovatoxin-a (OVTX-a) and of the structural isomers ovatoxin-d and -e (OVTX-d, -e). Enlargements of the full HRMS spectra of (B) OVTX-a and (C) OVTX-d/-e.

and *Coolia* as well as by other authors (Fraga et al. 2011, Mohammad-Noor et al. 2013, Fraga and Rodríguez 2014), arguing that, although this interpretation does not follow the strict relationships among the plates, it takes into account their homology, according to the tabulation of Gonyaulacales (Balech 1980, Fensome et al. 1993).

In this paper, we adopted the interpretation of the thecal plates used by Hoppenrath et al. (2014), who mainly followed the original description of Fukuyo (1981), Norris et al. (1985) and Faust et al. (1996) regarding the epitheca, and Besada et al. (1982) regarding the hypotheca, recognizing that there is no an intercalary plate in *Ostreopsis*. In this regard, we observed that the large hypothecal plate at the antapex contacts the Sp plate (and therefore the sulcus), although the contact area is very narrow and not always visible, confirming that is not an intercalary but an antapical plate (i.e., the $2''''$), as suggested by Hoppenrath et al. (2014). The uncertainty in the attribution of the large hypothetical plate (i.e., 1p vs. $1''''$) may be explained by the

TABLE 2. LC-HRMS analyses of *Ostreopsis fattorussoi* strains from Lebanon.

	Toxin content (pg · cell ⁻¹)	Relative intensities		
		OVTX-a	OVTX-d	OVTX-e
L1002	nd	—	—	—
L1007	0.28	81.6%	11.7%	6.7%
L1008	nd	—	—	—
L1020	0.47	86.7%	8.8%	4.5%
L1022	0.94	87.8%	7.7%	4.5%

TABLE 3. Different interpretations of plate tabulation in *Ostreopsis* of different authors. n.r., not reported.

	Besada et al. (1982), Escalera et al. (2015)	Norris et al. (1985), Faust et al. (1996)	Hoppenrath et al. (2014)
Epitheca	Po (pp) 4' 2' 3' 1' 1'' 2'' 3'' 4'' 5'' 6''	Po 1' 2' 3' 1'' 2'' 3'' 4'' 5'' 6'' 7''	Po 1' 2' 3' 1'' 2'' 3'' 4'' 5'' 6'' 7''
Hypotheca	1''' 2''' 3''' 4''' 5''' 1'''' 2''''	1''' 2''' 3''' 4''' 5''' 1'''' 1p	1''' 2''' 3''' 4''' 5''' 1'''' 2''''
Cingulum	n.r. n.r. n.r. n.r. n.r.	n.r. n.r. n.r. n.r. n.r.	1c 2c 3c 4c 5c
Sulcus	n.r. n.r. n.r. n.r. n.r. n.r. n.r. ps	n.r. n.r. n.r. n.r. n.r. n.r. n.r.	6c Sa Sda Ssa S.a.c.a Sdp Ssp Sp

contact point of this plate with the sulcus that may not be visible in some species (Hoppenrath et al. 2014), as also within the same species (Sato et al. 2011, Escalera et al. 2014).

O. fattorussoi could quickly be distinguished from the other two Mediterranean species in LM by its round thecal pores which are easily visible and appear larger than those in both *O. cf. ovata* and *O. cf. siamensis* (Table 4). Moreover, differently from *O. cf. ovata*, which shows pores of two size classes (Penna et al. 2005, Kang et al. 2013), pores of only one size class were visible in *O. fattorussoi*. Another way to distinguish *O. fattorussoi* from *O. cf. ovata* is the Po, which is longer in the former (Table 4). Moreover, the shape of the 6" plate is different: the 6"/5" suture length is almost twice as long as 6"/7" suture length, and the length:width ratio of the plate 6" is 1.06 ± 0.11 (0.95–1.2), while in *O. cf. siamensis* and *O. cf. ovata* is 1.5 ± 0.2 (1.1–2.4) and 1.6 ± 0.2 (1.3–2.1), respectively (David et al. 2013).

Moreover, *O. fattorussoi* is readily distinguishable from the other *Ostreopsis* species because of some peculiar characteristics of its plate tabulation (Fig. 11). (i) in *O. fattorussoi* the 1' plate lies in the left-half of the epitheca and is obliquely orientated giving a characteristic shape to the 6" plate and the oblique 6"/1' suture. In all other *Ostreopsis* species, the 1' plate closely occupies the center of the epitheca and is not oblique. (ii) *O. fattorussoi* is readily identifiable by the curved suture between 1' and 3' which makes plates 1' and 3' approximately hexagonal, while in the other *Ostreopsis* species they are pentagonal (with the exception of *Ostreopsis heptagona* which have a quadrangular 3' and a pentagonal 1' plate).

In *O. fattorussoi*, the 2' plate is narrow and almost twice the size of Po, separating the 3' and 3" plates. This characteristic could be useful to distinguish *O. fattorussoi* from many of the other *Ostreopsis* species, as only in *O. heptagona* and *O. labens* does plate 2' seem to divide plate 3' from plate 3" (Fig. 11). This characteristic may also be present in other *Ostreopsis* species but just not reported in their morphological descriptions: for example, in the original

description of *O. ovata*, Fukuyo (1981) indicated that this plate does not touch the plate 4", while this contact was indicated later by Besada et al. (1982). Similarly, *O. cf. ovata* has been described with (Selina and Orlova 2010, Kang et al. 2013) or without this contact (Escalera et al. 2014).

The hypotheca of *O. fattorussoi* does not show differences with that of *O. cf. ovata* (see Selina and Orlova 2010, Hoppenrath et al. 2014), although it does differ from the original drawings of *O. cf. ovata* by Fukuyo (1981) (e.g., the latter has smaller 1"" plate, a longer 2""/4"" suture, a longer and narrower 2"" plate and a smaller 3"").

The correct identification of *Ostreopsis* species in field samples based only on morphometric characters is often highly problematic. As the species recorded in Mediterranean Sea until now (*O. cf. ovata* and *O. cf. siamensis*) are very similar in shape and size, the DV/AP ratio was proposed as a characteristic for a quick distinction between the two species. Originally a DV/AP ratio of <2 for *O. cf. ovata* and >4 for *O. cf. siamensis* was proposed (Penna et al. 2005, Aligizaki and Nikolaidis 2006, Selina and Orlova 2010). The situation is now slightly more complex giving that *O. cf. ovata* from the northern Adriatic Sea was shown to have a DV/AP ratio slightly higher than 2, ~2.3–2.4 (Monti et al. 2007, Guerrini et al. 2010, Accoroni et al. 2012b). *O. fattorussoi* has a DV/AP ratio of 2.35 ± 0.22 μm so this character is of no use to discriminate between *O. fattorussoi* and *O. cf. ovata*.

Considering cell size, *O. fattorussoi* seems to be on average slightly bigger (DV: 60.1 ± 5.6 μm , AP: 25.7 ± 3 μm , W: 39.8 ± 5.1 μm) than *O. cf. ovata*, but these dimensions still fall within the upper range of the morphological variability reported for the latter species in natural samples (e.g., Accoroni et al. 2012b, Kang et al. 2013, Carnicer et al. 2015).

O. fattorussoi and *O. ovata* are the smallest species of the genus and misidentification in field samples, in case both were present, is likely. In this regard, David et al. (2013) who stated their difficulties in distinguishing on a morphological base *Ostreopsis* spp. in field samples, most likely showed

TABLE 4. Comparison of morphometric parameters of *Ostreopsis siamensis*, *O. ovata*, *O. cf. siamensis*, *O. cf. ovata*, and *O. fattorussoi* based on measurements of specimens from literature values and this study.

Species	Apical pore (μm)	Pore size in thecal plates (μm)	Reference
<i>O. fattorussoi</i> sp.nov.	10–12.5 (11.7 ± 1.4)	0.26–0.53 (0.38 ± 0.08)	This study
<i>O. siamensis</i> Schmidt	27	0.1–0.5	Faust et al. 1996,
		0.08–0.38	Chang et al. 2000,
<i>O. cf. siamensis</i>	7.4–9.7	0.11–0.56 (0.30 ± 0.07)	Penna et al. 2005,
	10.9 ± 1.24	0.23–0.29	Aligizaki and Nikolaidis 2006,
	11–13	0.14–0.32	Selina and Orlova 2010,
<i>O. ovata</i> Fukuyo	8	0.07	Faust et al. 1996,
	6.9–9.6	0.16–0.55 (0.34 ± 0.10)	Penna et al. 2005,
	10.9 ± 0.77	0.07–0.32	Aligizaki and Nikolaidis 2006,
<i>O. cf. ovata</i>	6.6–9.0	0.25	Monti et al. 2007,
	6.3–8.3	0.12–0.25	Selina and Orlova 2010,
	4.8–6.8	0.06–0.26	Kang et al. 2013

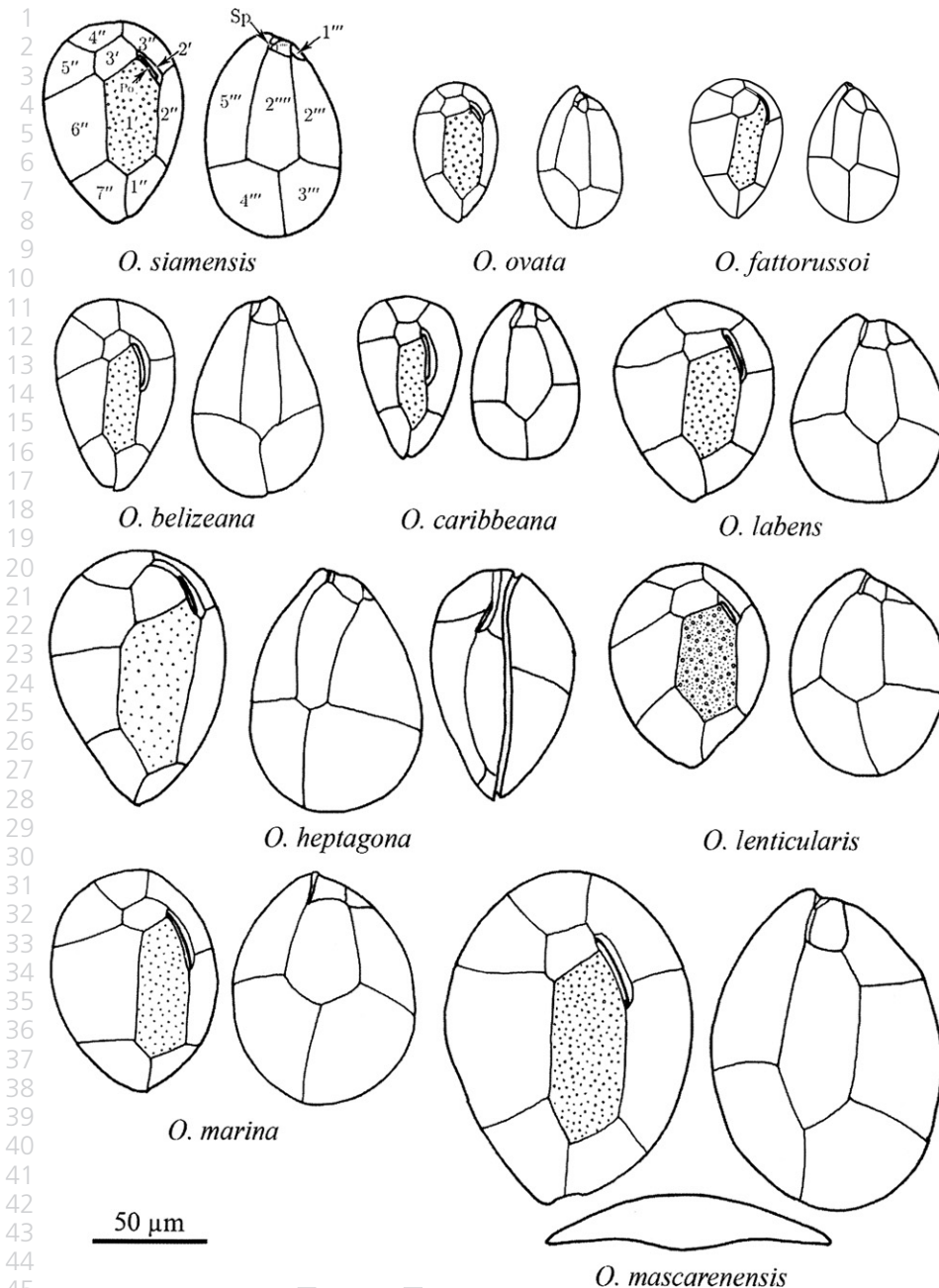


FIG. 11. Drawings of the plate patterns of the ten described *Ostreopsis* spp. modified from Hoppenrath et al. (2014). All species to scale.

47 *O. fattorussoi* and certainly not *O. cf. ovata* in their
48 Figure 6A, given both the oblique plate 1' and 1'/6"
49 suture and the wide thecal pores and Po. If true
50 then the distribution of *O. fattorussoi* is likely to
51 include the Atlantic section of the Iberian Penin-
52 sula.

53 The ITS-5.8S and D1/D2 LSU ribosomal genes
54 were able to consistently delineate divergences at
55 the species level among *Ostreopsis* species (Sato et al.
56 2011, David et al. 2013, Penna et al. 2014, Tawong
57 et al. 2014). In particular, the rDNA phylogeny
58 showed clearly that strains belonging to *O. fattorussoi*
59 were included in a distinct clade; in fact, both ITS-
60 5.8S and LSU rDNA tree topologies were very

similar. The phylogenetic inference obtained from
rDNA sequences was robust demonstrating that the
clade grouping *O. fattorussoi* strains was supported
by high values of bootstraps and Bayesian infer-
ences. Specifically, the ITS phylogeny indicated the
existence of *O. fattorussoi*, which included strains
from eastern Mediterranean and Atlantic, as sister
clade of *O. cf. siamensis*. The LSU phylogeny also
indicated the presence of *O. fattorussoi* as a distinct
species. This clade represented the second grouping
that segregated from the first one comprising *Ostre-*
opsis sp., *Ostreopsis* sp. 5, and *O. cf. lenticularis*. Fur-
thermore, collectively the rDNA phylogenies
indicated the existence of at least other six different

1 species (Sato et al. 2011, Penna et al. 2014, Tawong
2 et al. 2014).

3 This is the first report of *O. fattorusoi* in Lebanese
4 coastal waters. The same species (reported as *Ostreop-*
5 *opsis* sp.) has previously been reported in Cyprus
6 coastal waters by Tartaglione et al. (2015). Besides
7 Cyprus and Lebanon, molecular analyses revealed
8 that the same genotype was found in Crete, Canary
9 Islands (Spain) and Puerto Rico (USA) (Penna
10 et al. 2010, 2014, David et al. 2013).

11 In the coastal waters of Lebanon, records of *Ostreop-*
12 *opsis* species date back from 1979 (Abboud-Abi Saab
13 1989), and until now, the only reported species was
14 *O. siamensis*, which has been recorded between July
15 and September in the majority of the rocky coasts
16 (Abboud-Abi Saab et al. 2013). In this study, *Ostreop-*
17 *opsis* cells were detected throughout the year at the
18 Lebanese coastal site, differently from the strongly
19 seasonal trends observed in other Mediterranean
20 areas (Accoroni et al. 2016). Molecular quantitative
21 analysis by qPCR carried out in Lebanese samples
22 indicated that *O. fattorusoi* was the dominant (often
23 exclusive) *Ostreopsis* species, while the presence of
24 *O. cf. ovata* was almost negligible (Casabianca S. and
25 Penna A. pers. comm.). Abundances of *O. fattorusoi*
26 were two orders of magnitude lower than those of
27 *O. cf. ovata* recorded in other Mediterranean areas
28 during their summer-late summer blooms (e.g.,
29 Mangialajo et al. 2011, Accoroni et al. 2015). How-
30 ever, it should be noted that in our study, the sam-
31 pling was carried out mainly on *Corallina elongata*, a
32 red alga with calcified (and therefore heavy) thallus
33 that strongly influences the values of *Ostreopsis* abun-
34 dances when they are expressed as cells · g⁻¹ fw.
35 *Ostreopsis* maximum abundances were detected dur-
36 ing the warmest months with two blooming periods
37 in June–July and August. *Ostreopsis* blooms are gen-
38 erally summer events in temperate areas and maxi-
39 mum abundances are normally associated with the
40 highest recorded temperatures (e.g., Aligizaki and
41 Nikolaidis 2006, Mangialajo et al. 2008). However,
42 some exceptions have been detected in the north-
43 ern Adriatic Sea (Monti et al. 2007, Accoroni et al.
44 2012a) and the Sea of Japan (Selina et al. 2014),
45 where blooms develop and reach maximum abun-
46 dances at temperature values below the summer
47 maximum. Similarly, *O. fattorusoi* showed the high-
48 est abundances when temperature values were
49 between 27°C and 29.7°C, that is, lower than the
50 summer maximum (31.5°C). This would suggest
51 that other environmental factors besides tempera-
52 ture may affect the development of *Ostreopsis* abun-
53 dances. Several studies have provided increasing
54 evidence of a link between harmful algal events and
55 the nutrient enrichment of coastal waters (Glibert
56 and Burkholder 2006, Heisler et al. 2008, Glibert
57 et al. 2010). Although a correlation between *O. fat-*
58 *torussoi* abundances and nutrient concentrations was
59 not observed, a significant correlation was high-
60 lighted between *O. fattorussoi* growth rates and

phosphate concentrations. The link between an
influx of phosphorus-rich waters and higher net
growth rate of *O. cf. ovata* has already been recog-
nized in the northern Adriatic Sea (Accoroni et al.
2015).

Ostreopsis species have been shown to produce dif-
ferent toxins, mostly belonging to the palytoxin
group. Mediterranean *O. cf. ovata* strains produce
palytoxin analogs, such as isobaric palytoxin, OVTX
-a, b, c, d, e, f, g, and h (Ciminiello et al. 2010,
2012b, Scalco et al. 2012, Brissard et al. 2015,
García-Altarets et al. 2015). On the contrary, the
Mediterranean *O. cf. siamensis* strain was shown rela-
tively non-toxic, producing only sub-fg levels of paly-
toxin (Ciminiello et al. 2013).

Blooms of *Ostreopsis* are well known in the
Mediterranean Sea due to their effect on human
health, mainly following inhalation of seawater dro-
plets containing *Ostreopsis* cells or fragments and/or
aerosolized toxins (Gallitelli et al. 2005, Kermarec
et al. 2008, Tichadou et al. 2010, Del Favero et al.
2012, Casabianca et al. 2013, Ciminiello et al.
2014). The typical symptoms of *Ostreopsis* intoxica-
tion through aerosol and/or direct contact expo-
sure are broncho-constriction, dyspnoea, fever,
conjunctivitis, and skin irritations. Moreover, in the
Mediterranean Sea, *Ostreopsis* toxins were found to
contaminate seafood (Aligizaki et al. 2008, Cimi-
niello et al. 2015, Pelin et al. 2016). Several labora-
tory studies have shown that *Ostreopsis* exerts toxicity
also on several marine organisms, both invertebrates
and vertebrates (Faimali et al. 2012, Gorbi et al.
2012, 2013, Pagliara and Caroppo 2012, Carella
et al. 2015). So far, no reports of human intoxica-
tions have been reported from Lebanon coast
(Abboud-Abi Saab, pers. comm.).

Recently, Tartaglione et al. (2015) described the
toxin profile of *Ostreopsis* sp. (named now as *O. fat-*
torussoi) isolated from Cyprus waters, showing some
strains to produce isobaric palytoxin and OVTX-a, d
and e, previously found only in *O. cf. ovata*, while
some others produced only new palytoxin-like com-
pounds named OVTX-i, OVTX-j₁, OVTX-j₂, and
OVTX-k. In this study, we showed that two of the five
analyzed Lebanese strains of *O. fattorussoi* were not
toxic, and three produced OVTX-a and the structural
isomers OVTX-d and -e. The confirmation for the
identity of these toxins was provided by their perfectly
superimposable LC-HRMS² spectra over those of pre-
viously characterized OVTX-a, -d, and -e (Ciminiello
et al. 2010, 2012a, Dell'Aversano et al. 2015). The
toxin profile of these strains also matched those of
other *O. fattorussoi* strains from Cyprus (Tartaglione
et al. 2015) and those found in ~40% of the Mediter-
ranean *O. cf. ovata* strains analyzed so far (Dell'Aver-
sano et al. 2015). However, Lebanese *O. fattorussoi*
strains analyzed here did not produce any new paly-
toxin-like compounds such as those found in Cypriot
O. fattorussoi (OVTX-i, OVTX-j₁, OVTX-j₂, and
OVTX-k, Tartaglione et al. 2015).

1 So far, the toxin content of *O. fattorussoi* strains
 2 has occurred in the range of 0.06–2.8 pg · cell⁻¹
 3 (Cyprus strains, Tartaglione et al. 2015 and Leba-
 4 nese strains, this study) which is significantly lower
 5 than that of the Mediterranean *O. cf. ovata* strains
 6 maintained in the same cultured conditions (up to
 7 44.0 pg · cell⁻¹, Tartaglione et al. 2015). This has
 8 also been further supported by eco-toxicological
 9 tests on *Artemia salina* nauplii showing that *O. fat-*
 10 *torussoi* from Cyprus had very low toxicity compared
 11 to *O. cf. ovata* (Tartaglione et al. 2015).

12 In conclusion, despite of the difficulties often
 13 reported concerning the identification of *Ostreopsis*
 14 species based on morphological characters alone
 15 (Penna et al. 2005, Parsons et al. 2012, David et al.
 16 2013), *O. fattorussoi* does show some morphological
 17 features that lead unequivocally to its identification.
 18 These include:

- 19 1 the curved suture between plate 1' and 3' which
- 20 makes plates them approximately hexagonal.
- 21 2 the 1' plate that lies in the left-half of the
- 22 epitheca and is obliquely orientated
- 23 3 the characteristic shape of plate 6'': its length:
- 24 width ratio of 1.06 ± 0.11 (0.95–1.2) and the
- 25 6''/5'' suture length is almost twice as long as
- 26 that of 6''/7'.
- 27

28 Moreover, the phylogenetic analyses show that
 29 *O. fattorussoi* belongs to the Atlantic/Mediterranean
 30 *Ostreopsis* spp. clade distinct from the other *Ostreopsis*
 31 species.

32 This benthic dinoflagellate has been detected
 33 along the Lebanon coast throughout the year 2015
 34 (with temperatures ranging from 18°C to 31.5°C),
 35 with bloom occurring in June and August and a sig-
 36 nificant correlation was highlighted between *Ostreop-*
 37 *sis* growth rates and phosphate concentrations.

38 *O. fattorussoi* is a toxic species producing OVTX-a
 39 and structural isomers OVTX-d and -e, so far found
 40 only in *O. cf. ovata*, and three exclusive palytoxin-
 41 like compounds (OVTX-i, OVTX-j₁, OVTX-j₂, and
 42 OVTX-k, Tartaglione et al. 2015). All the data col-
 43 lected on this new species about its toxicity so far,
 44 however, would suggest a lower risk to human
 45 health and marine fauna to that of *O. cf. ovata*.

46 We gratefully acknowledge Demetris Kletou for the help in
 47 collecting Cyprus samples, Antonia Mazzeo for her assistance
 48 with the chemical analysis of toxins and Silvia Casabianca for
 49 molecular information about Lebanese *Ostreopsis* occurrence.
 50 A special thanks to Neil T.W. Ellwood for the English revision.
 51 This publication has been produced with the financial
 52 assistance of the European Union under the ENPI CBC MED
 53 Programme (M3-HABs project). The LC-HRMS study was
 54 granted by Programme STAR Linea 1 2013 (VALTOX,
 55 Napoli_call2013_08) financially supported by UniNA and
 56 Compagnia di San Paolo.

57 Abboud-Abi Saab, M. 1989. Les Dinoflagellés des eaux côtières
 58 libanaises. Espèces rares ou nouvelles du phytoplancton
 59 marin. *Leb. Sci. Bull.* 5:5–16.

Abboud-Abi Saab, M., Fakhri, M., Kassab, M.-T. & Matar, N. 2013. Seasonal and spatial variations of the dinoflagellate *Ostreopsis siamensis* in the Lebanese coastal waters (Eastern Mediterranean). *Cryptogamie Algol.* 34:57–67.

Accoroni, S., Colombo, F., Pichierrri, S., Romagnoli, T., Marini, M., Battocchi, C., Penna, A. & Totti, C. 2012a. Ecology of *Ostreopsis cf. ovata* blooms in the northwestern Adriatic Sea. *Cryptogamie Algol.* 33:191–8.

Accoroni, S., Glibert, P. M., Pichierrri, S., Romagnoli, T., Marini, M. & Totti, C. 2015. A conceptual model of annual *Ostreopsis cf. ovata* blooms in the northern Adriatic Sea based on the synergic effects of hydrodynamics, temperature, and the N:P ratio of water column nutrients. *Harmful Algae* 45:14–25.

Accoroni, S., Romagnoli, T., Colombo, F., Pennesi, C., Di Camillo, C. G., Marini, M., Battocchi, C. et al. 2011. *Ostreopsis cf. ovata* bloom in the northern Adriatic Sea during summer 2009: ecology, molecular characterization and toxin profile. *Mar. Pollut. Bull.* 62:2512–9.

Accoroni, S., Romagnoli, T., Pichierrri, S., Colombo, F. & Totti, C. 2012b. Morphometric analysis of *Ostreopsis cf. ovata* cells in relation to environmental conditions and bloom phases. *Harmful Algae* 19:15–22.

Accoroni, S., Romagnoli, T., Pichierrri, S. & Totti, C. 2016. Effects of the bloom of harmful benthic dinoflagellate *Ostreopsis cf. ovata* on the microphytobenthos community in the northern Adriatic Sea. *Harmful Algae* 55:179–90.

Accoroni, S. & Totti, C. 2016. The toxic benthic dinoflagellates of the genus *Ostreopsis* in temperate areas: a review. *Adv. Oceanogr. Limnol.* 7:1–15.

Aligizaki, K., Katikou, P., Nikolaidis, G. & Panou, A. 2008. First episode of shellfish contamination by palytoxin-like compounds from *Ostreopsis* species (Aegean Sea, Greece). *Toxicol.* 51:418–27.

Aligizaki, K. & Nikolaidis, G. 2006. The presence of the potentially toxic genera *Ostreopsis* and *Coolia* (Dinophyceae) in the north Aegean Sea, Greece. *Harmful Algae* 5:717–30.

Amorim, A., Veloso, V. & Penna, A. 2010. First detection of *Ostreopsis cf. siamensis* in Portuguese coastal waters. *Harmful Algae News* 42:6–7.

Balech, E. 1980. On thecal morphology of dinoflagellates with special emphasis on circular and sulcal plates. *An. Centro Cienc. Mar. Limnol. Univ. Nat. Autóm. México* 7:57–68.

Battocchi, C., Totti, C., Vila, M., Masó, M., Capellacci, S., Accoroni, S., Reñé, A., Scardi, M. & Penna, A. 2010. Monitoring toxic microalgae *Ostreopsis* (dinoflagellate) species in coastal waters of the Mediterranean Sea using molecular PCR-based assay combined with light microscopy. *Mar. Pollut. Bull.* 60:1074–84.

Bennouna, A., El Attar, J., Abouabdellah, R., Palma, S., Penna, A. & Moita, T. 2010. First records of *Ostreopsis cf. siamensis* in Moroccan Atlantic upwelling waters. *Harmful Algae News* 42:1–3.

Besada, E. G., Loeblich, L. A. & Loeblich, A. R. 1982. Observations on tropical, benthic dinoflagellates from ciguatera-endemic areas - *Coolia*, *Gambierdiscus* and *Ostreopsis*. *Bull. Mar. Sci.* 32:723–35.

Bomber, J. W. & Aikman, K. E. 1989. The ciguatera dinoflagellates. *Biological Oceanography* 6:291–311.

Bravo, I., Vila, M., Casabianca, S., Rodriguez, F., Rial, P., Riobó, P. & Penna, A. 2012. Life cycle stages of the benthic palytoxin-producing dinoflagellate *Ostreopsis cf. ovata* (Dinophyceae). *Harmful Algae* 18:24–34.

Brissard, C., Hervé, F., Sibat, M., Séchet, V., Hess, P., Amzil, Z. & Herrenknecht, C. 2015. Characterization of ovatoxin-h, a new ovatoxin analog, and evaluation of chromatographic columns for ovatoxin analysis and purification. *J. Chromatogr. A* 1388:87–101.

Carella, F., Sardo, A., Mangoni, O., Di Cioccio, D., Urciuolo, G., De Vico, G. & Zingone, A. 2015. Quantitative histopathology of the Mediterranean mussel (*Mytilus galloprovincialis* L.) exposed to the harmful dinoflagellate *Ostreopsis cf. ovata*. *J. Invertebr. Pathol.* 127:130–40.

- Carlson, R. D. & Tindall, D. R. 1985. Distribution and periodicity of toxic dinoflagellates in the Virgin Islands. In Anderson, D. M., White, A. W. & Baden, D. G. [Eds.] *Toxic Dinoflagellates*. Elsevier, Amsterdam, the Netherlands, pp. 171–6.
- Carnicer, O., Guallar, C., Andree, K. B., Diogène, J. & Fernández-Tejedor, M. 2015. *Ostreopsis* cf. *ovata* dynamics in the NW Mediterranean Sea in relation to biotic and abiotic factors. *Environ. Res.* 143(Part B):89–99.
- Casabianca, S., Casabianca, A., Riobó, P., Franco, J. M., Vila, M. & Penna, A. 2013. Quantification of the toxic dinoflagellate *Ostreopsis* spp. by qPCR assay in marine aerosol. *Environ. Sci. Technol.* 47:3788–95.
- Chang, F. H., Shimizu, Y., Hay, B., Stewart, R., Mackay, G. & Tasker, R. 2000. Three recently recorded *Ostreopsis* spp. (Dinophyceae) in New Zealand: temporal and regional distribution in the upper North Island from 1995 to 1997. *New Zeal. J. Mar. Fresh.* 34:29–39.
- Ciminiello, P., Dell'Aversano, C., Dello Iacovo, E., Fattorusso, E., Forino, M., Grauso, L. & Tartaglione, L. 2012a. High resolution LC-MSn fragmentation pattern of palytoxin as template to gain new insights into ovatoxin-A structure. The key role of calcium in MS behavior of palytoxins. *J. Am. Soc. Mass Spectr.* 23:952–63.
- Ciminiello, P., Dell'Aversano, C., Dello Iacovo, E., Fattorusso, E., Forino, M., Grauso, L., Tartaglione, L., Guerrini, F. & Pistocchi, R. 2010. Complex palytoxin-like profile of *Ostreopsis ovata*. Identification of four new ovatoxins by high-resolution liquid chromatography/mass spectrometry. *Rapid Commun. Mass Sp.* 24:2735–44.
- Ciminiello, P., Dell'Aversano, C., Dello Iacovo, E., Fattorusso, E., Forino, M., Tartaglione, L., Battocchi, C. & Penna, A. 2012b. Unique toxin profile of a Mediterranean *Ostreopsis* cf. *ovata* strain: HR LC-MSn characterization of ovatoxin-f, a new palytoxin congener. *Chem. Res. Toxicol.* 25:1243–52.
- Ciminiello, P., Dell'Aversano, C., Dello Iacovo, E., Fattorusso, E., Forino, M., Tartaglione, L., Benedettini, G. et al. 2014. First finding of *Ostreopsis* cf. *ovata* toxins in marine aerosols. *Environ. Sci. Technol.* 48:3532–40.
- Ciminiello, P., Dell'Aversano, C., Dello Iacovo, E., Forino, M. & Tartaglione, L. 2015. Liquid chromatography–high-resolution mass spectrometry for palytoxins in mussels. *Anal. Bioanal. Chem.* 407:1463–73.
- Ciminiello, P., Dell'Aversano, C., Fattorusso, E., Forino, M., Magno, G. S., Tartaglione, L., Grillo, C. & Melchiorre, N. 2006. The Genoa 2005 outbreak. Determination of putative palytoxin in Mediterranean *Ostreopsis ovata* by a new liquid chromatography tandem mass spectrometry method. *Anal. Chem.* 78:6153–9.
- Ciminiello, P., Dell'Aversano, C., Iacovo, E. D., Fattorusso, E., Forino, M., Tartaglione, L., Yasumoto, T., Battocchi, C., Giacobbe, M., Amorim, A. & Penna, A. 2013. Investigation of toxin profile of Mediterranean and Atlantic strains of *Ostreopsis* cf. *siamensis* (Dinophyceae) by liquid chromatography–high resolution mass spectrometry. *Harmful Algae* 23:19–27.
- Coats, D. W. 2002. Dinoflagellate life-cycle complexities. *J. Phycol.* 38:417–9.
- Cohu, S., Mangialajo, L., Thibaut, T., Blanfuné, A., Marro, S. & Lemée, R. 2013. Proliferation of the toxic dinoflagellate *Ostreopsis* cf. *ovata* in relation to depth, biotic substrate and environmental factors in the North West Mediterranean Sea. *Harmful Algae* 24:32–44.
- Darriba, D., Taboada, G. L., Doallo, R. & Posada, D. 2012. jModelTest 2: more models, new heuristics and parallel computing. *Nat. Methods* 9:772.
- David, H., Laza-Martinez, A., Miguel, I. & Orive, E. 2013. *Ostreopsis* cf. *siamensis* and *Ostreopsis* cf. *ovata* from the Atlantic Iberian Peninsula: morphological and phylogenetic characterization. *Harmful Algae* 30:44–55.
- Del Favero, G., Sosa, S., Pelin, M., D'Orlando, E., Florio, C., Lorenzon, P., Poli, M. & Tubaro, A. 2012. Sanitary problems related to the presence of *Ostreopsis* spp. in the Mediterranean Sea: a multidisciplinary scientific approach. *Ann Ist Super Sanità* 48:407–14.
- Dell'Aversano, C., Tartaglione, L., Dello Iacovo, E., Forino, M., Casabianca, S., Penna, A. & Ciminiello, P. 2015. *Ostreopsis* cf. *ovata* from the Mediterranean Sea. Variability in toxin profiles and structural elucidation of unknowns through LC-HRMSⁿ. In MacKenzie, A. L. [Ed.] *Marine and Freshwater Harmful Algae. Proceedings of the 16th International Conference on Harmful Algae, Wellington, New Zealand 27th-31st October 2014*. Cawthron Institute, Nelson, New Zealand and International Society for the Study of Harmful Algae (ISSHA), ISBN 978-87-990827-5-9; pp. 70–3.
- Edler, L. & Elbrachter, M. 2010. The Utermöhl method for quantitative phytoplankton analysis. In Karlson, B., Cusack, C. & Bresnan, E. [Eds.] *Microscopic and Molecular Methods for Quantitative Phytoplankton Analysis*. UNESCO, Paris (IOC Manuals and Guides, no. 55), pp. 13–20.
- Escalera, L., Benvenuto, G., Scalco, E., Zingone, A. & Montresor, M. 2014. Ultrastructural features of the benthic dinoflagellate *Ostreopsis* cf. *ovata* (Dinophyceae). *Protist* 165:260–74.
- Faimali, M., Giussani, V., Piazza, V., Garaventa, F., Corrà, C., Asnaghi, V., Privitera, D., Gallus, L., Cattaneo-Vietti, R., Mangialajo, L. & Chiantore, M. 2012. Toxic effects of harmful benthic dinoflagellate *Ostreopsis ovata* on invertebrate and vertebrate marine organisms. *Mar. Environ. Res.* 76:97–107.
- Faust, M. A. 1999. Three new *Ostreopsis* species (Dinophyceae): *O. marinus* sp. nov., *O. belizeanus* sp. nov., and *O. carribeanus* sp. nov. *Phycologia* 38:92–9.
- Faust, M. A. & Morton, S. L. 1995. Morphology and ecology of the marine dinoflagellate *Ostreopsis labens* sp. nov. (Dinophyceae). *J. Phycol.* 31:456–63.
- Faust, M. A., Morton, S. L. & Quod, J. P. 1996. Further SEM study of marine dinoflagellates: the genus *Ostreopsis* (Dinophyceae). *J. Phycol.* 32:1053–65.
- Fensome, R. A., Taylor, F. J. R., Norris, G., Sarjeant, W. A. S., Wharton, D. I. & Williams, G. L. 1993. *A Classification of Living and Fossil Dinoflagellates*. Micropaleontology, Special Publication Number 7. Sheridan Press, Hanover, Pennsylvania, 351 pp.
- Fraga, S. & Rodríguez, F. 2014. Genus *Gambierdiscus* in the Canary Islands (NE Atlantic Ocean) with description of *Gambierdiscus silvae* sp. nov., a new potentially toxic epiphytic benthic dinoflagellate. *Protist* 165:839–53.
- Fraga, S., Rodríguez, F., Caillaud, A., Diogene, J., Raho, N. & Zapata, M. 2011. *Gambierdiscus excentricus* sp. nov. (Dinophyceae), a benthic toxic dinoflagellate from the Canary Islands (NE Atlantic Ocean). *Harmful Algae* 11:10–22.
- Fukuyo, Y. 1981. Taxonomical study on benthic dinoflagellates collected in coral reefs. *Bull. Jap. Soc. Sci. Fish.* 47:967–78.
- Gallitelli, M., Ungaro, N., Addante, L. M., Silver, N. G. & Sabba, C. 2005. Respiratory illness as a reaction to tropical algal blooms occurring in a temperate climate. *J. Am. Med. Assoc.* 293:2599–600.
- García-Altare, M., Tartaglione, L., Dell'Aversano, C., Carnicer, O., De La Iglesia, P., Forino, M., Diogène, J. & Ciminiello, P. 2015. The novel ovatoxin-g and isobaric palytoxin (so far referred to as putative palytoxin) from *Ostreopsis* cf. *ovata* (NW Mediterranean Sea): structural insights by LC-high resolution MSⁿ. *Anal. Bioanal. Chem.* 407:1191–204.
- Giussani, V., Sbrana, F., Asnaghi, V., Vassalli, M., Faimali, M., Casabianca, S., Penna, A. et al. 2015. Active role of the mucilage in the toxicity mechanism of the harmful benthic dinoflagellate *Ostreopsis* cf. *ovata*. *Harmful Algae* 44:46–53.
- Glibert, P. M., Allen, J. I., Bouwman, A. F., Brown, C. W., Flynn, K. J., Lewitus, A. J. & Madden, C. J. 2010. Modeling of HABs and eutrophication Status, advances, challenges. *J. Marine Syst.* 83:262–75.
- Glibert, P. M. & Burkholder, J. M. 2006. The complex relationships between increases in fertilization of the earth, coastal eutrophication and proliferation of Harmful Algal Blooms. In Granéli, E. & Turner, J. T. [Eds.] *Ecology of Harmful Algae*. Springer Berlin Heidelberg, Heidelberg, Germany, pp. 341–54.
- Gorbi, S., Avio, G. C., Benedetti, M., Totti, C., Accoroni, S., Pichierri, S., Bacchiocchi, S., Orletti, R., Graziosi, T. &

- Regoli, F. 2013. Effects of harmful dinoflagellate *Ostreopsis* cf. *ovata* exposure on immunological, histological and oxidative responses of mussels *Mytilus galloprovincialis*. *Fish Shellfish Immun.* 35:941–50.
- Gorbi, S., Bocchetti, R., Binelli, A., Bacchiocchi, S., Orletti, R., Nanetti, L., Raffaelli, F., Vignini, A., Accoroni, S., Totti, C. & Regoli, F. 2012. Biological effects of palytoxin-like compounds from *Ostreopsis* cf. *ovata*: a multibiomarkers approach with mussels *Mytilus galloprovincialis*. *Chemosphere* 89:623–32.
- Guerrini, F., Pezzolesi, L., Feller, A., Riccardi, M., Ciminiello, P., Dell'Aversano, C., Tartaglione, L., Dello Iacovo, E., Fattorusso, E., Forino, M. & Pistocchi, R. 2010. Comparative growth and toxin profile of cultured *Ostreopsis ovata* from the Tyrrhenian and Adriatic Seas. *Toxicon* 55:211–20.
- Guillard, R. R. L. 1975. Culture of phytoplankton for feeding marine invertebrates. In Smith, W. L. & Chanley, M. H. [Eds.] *Culture of Marine Invertebrates Animals*. Plenum Press, New York, pp. 26–60.
- Guillard, R. R. L. 1978. Counting slides. In Sourmia, A. [Ed.] *Phytoplankton Manual. Monographs on Oceanographic Methodology* 6. UNESCO, Paris, pp. 182–9.
- Guindon, S., Dufayard, J. F., Lefort, V., Anisimova, M., Hordijk, W. & Gascuel, O. 2010. New algorithms and methods to estimate maximum-likelihood phylogenies, assessing the performance of PhyML 3.0. *Syst. Biol.* 59:307–21.
- Heisler, J., Glibert, P. M., Burkholder, J. M., Anderson, D. M., Cochlan, W., Dennison, W. C., Dortch, Q. et al. 2008. Eutrophication and harmful algal blooms: a scientific consensus. *Harmful Algae* 8:3–13.
- Holmes, M. J., Gillespie, N. C. & Lewis, R. J. 1988. Toxicity and morphology of *Ostreopsis* cf. *siamensis* cultured from a ciguatera endemic region of Queensland, Australia. In Choat, J. H., Barnes, D., Borowitzka, M. A., Coll, J. C., Davies, P. J., Flood, P., Hatcher, B. G., Hopley, D., Hutchings, P. A., Kinsey, D., Orme, G. R., Pichon, M., Sale, P. F., Sammarco, P., Wallace, C. C., Wilkinson, C., Wolanski, E. & Bellwood, O. [Eds.] *Proceedings of the 6th International Coral Reef Symposium*. ?????, Townsville, Australia, pp. 49–54.
- Hoppenrath, M., Murray, S. A., Chomérat, N. & Horiguchi, T. 2014. *Marine Benthic Dinoflagellates - Unveiling their Worldwide Biodiversity*. Kleine Senckenberg-Reihe, Band 54, Schweizerbart, Stuttgart, Germany, 276 pp.
- Hoshaw, R. W. & Rosowski, J. R. 1973. Methods for microscopic algae. In Stein, J. R. [Ed.] *Handbook of Phycological Methods*. Cambridge University Press, New York, pp. 53–67.
- Illoul, H., Hernandez, F. R., Vila, M., Adjias, N., Younes, A. A., Bourmissa, M., Koroghli, A., Marouf, N., Rabia, S. & Ameer, F. L. K. 2012. The genus *Ostreopsis* along the Algerian coastal waters (SW Mediterranean Sea) associated with a human respiratory intoxication episode. *Cryptogam. Algologie* 33:209–16.
- Ismael, A. & Halim, Y. 2012. Potentially harmful *Ostreopsis* spp. In the coastal waters of Alexandria-Egypt. *Mediterr. Mar. Sci.* 13:208–12.
- Kang, N. S., Jeong, H. J., Lee, S. Y., Lim, A. S., Lee, M. J., Kim, H. S. & Yih, W. 2013. Morphology and molecular characterization of the epiphytic benthic dinoflagellate *Ostreopsis* cf. *ovata* in the temperate waters off Jeju Island, Korea. *Harmful Algae* 27:98–112.
- Kermarec, F., Dor, F., Armengaud, A., Charlet, F., Kantin, R., Sauzade, D. & De Haro, L. 2008. Les risques sanitaires liés à la présence d'*Ostreopsis ovata* dans les eaux de baignade ou d'activités nautiques. *Environnement, Risques & Santé* 7:357–63.
- Laza-Martinez, A., Orive, E. & Miguel, I. 2011. Morphological and genetic characterization of benthic dinoflagellates of the genera *Coolia*, *Ostreopsis* and *Prorocentrum* from the south-eastern Bay of Biscay. *Eur. J. Phycol.* 46:45–65.
- Lenoir, S., Ten-Hage, L., Turquet, J., Quod, J. P., Bernard, C. & Hennion, M. C. 2004. First evidence of palytoxin analogues from an *Ostreopsis marseillensis* (Dinophyceae) benthic bloom in Southwestern Indian Ocean. *J. Phycol.* 40:1042–51.
- Litaker, R. W., Vandersea, M. W., Faust, M. A., Kibler, S. R., Chinnain, M., Holmes, M. J., Holland, W. C. & Tester, P. A. 2009. Taxonomy of *Gambierdiscus* including four new species, *Gambierdiscus caribaeus*, *Gambierdiscus carolinianus*, *Gambierdiscus carpenteri* and *Gambierdiscus ruetzleri* (Gonyaulacales, Dinophyceae). *Phycologia* 48:344–90.
- Mabrouk, L., Hamza, A., Brahim, M. B. & Bradai, M. N. 2011. Temporal and depth distribution of microepiphytes on *Posidonia oceanica* (L.) Delile leaves in a meadow off Tunisia. *Mar. Ecol. Evol. Persp.* 32:148–61.
- Mabrouk, L., Hamza, A., Mahfoudi, M. & Bradai, M. N. 2012. Spatial and temporal variations of epiphytic *Ostreopsis siamensis* on *Posidonia oceanica* (L.) Delile leaves in Mahdia (Tunisia). *Cah. Biol. Mar.* 53:419–27.
- Mangialajo, L., Bertolotto, R., Cattaneo-Vietti, R., Chiantore, M., Grillo, C., Lemée, R., Melchiorre, N., Moretto, P., Povero, P. & Ruggieri, N. 2008. The toxic benthic dinoflagellate *Ostreopsis ovata*: quantification of proliferation along the coastline of Genoa, Italy. *Mar. Pollut. Bull.* 56:1209–14.
- Mangialajo, L., Ganzin, N., Accoroni, S., Asnaghi, V., Blanfuné, A., Cabrini, M., Cattaneo-Vietti, R. et al. 2011. Trends in *Ostreopsis* proliferation along the Northern Mediterranean coasts. *Toxicon* 57:408–20.
- Mercado, J. A., Rivera-Rentas, A. L., Gonzalez, I., Tosteson, T. R., Molgo, J. & Escalona de Motta, G. 1994. Neuro- and myo-toxicity of extracts from the benthic dinoflagellate *Ostreopsis lenticularis* is sensitive to μ -conotoxin. *Soc. Neurosci. Abstr.* 20:718.
- Meunier, F. A., Mercado, J. A., Molgó, J., Tosteson, T. R. & Escalona de Motta, G. 1997. Selective depolarization of the muscle membrane in frog nerve-muscle preparations by a chromatographically purified extract of the dinoflagellate *Ostreopsis lenticularis*. *Brit. J. Pharmacol.* 121:1224–30.
- Mohammad-Noor, N., Moestrup, Ø., Lundholm, N., Fraga, S., Adam, A., Holmes, M. J. & Saleh, E. 2013. Autecology and phylogeny of *Coolia tropicalis* and *Coolia malayensis* (Dinophyceae), with emphasis on taxonomy of *C. tropicalis* based on light microscopy, scanning electron microscopy and LSU rDNA. *J. Phycol.* 49:536–45.
- Monti, M., Minocci, M., Beran, A. & Ivesa, L. 2007. First record of *Ostreopsis* cf. *ovata* on macroalgae in the Northern Adriatic Sea. *Mar. Pollut. Bull.* 54:598–601.
- Murphy, J. & Riley, J. P. 1962. A modified single solution method for the determination of phosphate in natural waters. *Anal. Chim. Acta* 27:31–6.
- Nakajima, I., Oshima, Y. & Yasumoto, T. 1981. Toxicity of benthic dinoflagellates in Okinawa. *Nippon Suisan Gakk.* 47:1029–33.
- Nascimento, S. M., Corrêa, E. V., Menezes, M., Varela, D., Paredes, J. & Morris, S. 2012. Growth and toxin profile of *Ostreopsis* cf. *ovata* (Dinophyta) from Rio de Janeiro, Brazil. *Harmful Algae* 13:1–9.
- Norris, D. R., Bomber, J. W. & Balech, E. 1985. Benthic dinoflagellates associated with ciguatera from Florida Keys. I. *Ostreopsis heptagona* sp. nov. In Anderson, D. M., White, A. W. & Baden, D. G. [Eds.] *Toxic Dinoflagellates*. Elsevier, Amsterdam, the Netherlands, pp. 39–44.
- Pagliara, P. & Caroppo, C. 2012. Toxicity assessment of *Amphidinium carterae*, *Coolia* cf. *monotis* and *Ostreopsis* cf. *ovata* (Dinophyta) isolated from the northern Ionian Sea (Mediterranean Sea). *Toxicon* 60:1203–14.
- Parsons, M. L., Aligizaki, K., Bottein, M.-Y. D., Fraga, S., Morton, S. L., Penna, A. & Rhodes, L. 2012. *Gambierdiscus* and *Ostreopsis*: reassessment of the state of knowledge of their taxonomy, geography, ecophysiology, and toxicology. *Harmful Algae* 14:107–29.
- Parsons, M. L. & Preskitt, L. B. 2007. A survey of epiphytic dinoflagellates from the coastal waters of the island of Hawai'i. *Harmful Algae* 6:658–69.
- Pearce, I., Marshall, J. A. & Hallegraef, G. 2001. Toxic epiphytic dinoflagellates from east coast Tasmania, Australia. In Hallegraef, G., Blackburn, S. I., Bolch, C. J. & Lewis, R. J. [Eds.] *Harmful Algal Blooms 2000*. Intergovernmental Oceanographic Commission of UNESCO, Paris, France, pp. 54–7.
- Pelin, M., Forino, M., Brovedani, V., Tartaglione, L., Dell'Aversano, C., Pistocchi, R., Poli, M., Sosa, S., Florio, C., Ciminiello, P. & Tubaro, A. 2016. Ovatoxin-a, a palytoxin

- analogue isolated from *Ostreopsis* cf. *ovata* Fukuyo: cytotoxic activity and ELISA detection. *Environ. Sci. Technol.* 50:1544–51.
- Penna, A., Battocchi, C., Capellacci, S., Fraga, S., Aligizaki, K., Lemée, R. & Vernesi, C. 2014. Mitochondrial, but not rDNA, genes fail to discriminate dinoflagellate species in the genus *Ostreopsis*. *Harmful Algae* 40:40–50.
- Penna, A., Fraga, S., Battocchi, C., Casabianca, S., Giacobbe, M. G., Riobó, P. & Vernesi, C. 2010. A phylogeographical study of the toxic benthic dinoflagellate genus *Ostreopsis* Schmidt. *J. Biogeogr.* 37:830–41.
- Penna, A., Fraga, S., Battocchi, C., Casabianca, S., Perini, F., Samuela, C., Casabianca, A. et al. 2012. Genetic diversity of the genus *Ostreopsis* Schmidt: phylogeographical considerations and molecular methodology applications for field detection in the Mediterranean Sea. *Cryptogamie Algol.* 33:153–63.
- Penna, A. & Galluzzi, L. 2013. The quantitative real-time PCR applications in the monitoring of marine harmful algal bloom (HAB) species. *Environ. Sci. Pollut. Res. Int.* 20:6851–62.
- Penna, A., Vila, M., Fraga, S., Giacobbe, M. G., Andreoni, F., Riobó, P. & Vernesi, C. 2005. Characterization of *Ostreopsis* and *Coolia* (Dinophyceae) isolates in the western Mediterranean Sea based on morphology, toxicity and internal transcribed spacer 5.8s rDNA sequences. *J. Phycol.* 41:212–25.
- Percopo, I., Siano, R., Rossi, R., Soprano, V., Sarno, D. & Zingone, A. 2013. A new potentially toxic *Azadinium* species (Dinophyceae) from the Mediterranean Sea, *A. dexteroporum* sp. nov.. *J. Phycol.* 49:950–66.
- Perini, F., Casabianca, A., Battocchi, C., Accoroni, S., Totti, C. & Penna, A. 2011. New approach using the real-time PCR method for estimation of the toxic marine dinoflagellate *Ostreopsis* cf. *ovata* in marine environment. *PLoS ONE* 6: e17699.
- Pfannkuchen, M., Godrijan, J., Maric Pfannkuchen, D., Ivesa, L., Krusic, P., Ciminiello, P., Dell'Aversano, C. et al. 2012. Toxin-producing *Ostreopsis* cf. *ovata* are likely to bloom undetected along coastal areas. *Environ. Sci. Technol.* 46:5574–82.
- Quod, J. P. 1994. *Ostreopsis mascarenensis* sp. nov. (Dinophyceae), dinoflagellé toxique associé à la ciguatera dans l'Océan Indien. *Cryptogamie Algol.* 15:243–51.
- Rhodes, L., Adamson, J., Suzuki, T., Briggs, L. & Garthwaite, I. 2000. Toxic marine epiphytic dinoflagellates, *Ostreopsis siamensis* and *Coolia monotis* (Dinophyceae), in New Zealand. *New Zeal. J. Mar. Fresh.* 34:371–83.
- Ronquist, F. & Huelsenbeck, J. P. 2003. MrBayes 3: Bayesian phylogenetic inference under mixed models. *Bioinformatics* 19:1572–4.
- Sato, S., Nishimura, T., Uehara, K., Sakanari, H., Tawong, W., Hariganeya, N., Smith, K. et al. 2011. Phylogeography of *Ostreopsis* along west Pacific coast, with special reference to a novel clade from Japan. *PLoS ONE* 6:e27983.
- Scalco, E., Brunet, C., Marino, F., Rossi, R., Soprano, V., Zingone, A. & Montresor, M. 2012. Growth and toxicity responses of Mediterranean *Ostreopsis* cf. *ovata* to seasonal irradiance and temperature conditions. *Harmful Algae* 17:25–34.
- Schmidt, J. 1901. Flora of Koh Chang. Contributions to the knowledge of the vegetation in the Gulf of Siam. *Peridiniales. Bot. Tidsskr.* 24:212–21.
- Selina, M. S., Morozova, T. V., Vyshkvartsev, D. I. & Orlova, T. Y. 2014. Seasonal dynamics and spatial distribution of epiphytic dinoflagellates in Peter the Great Bay (Sea of Japan) with special emphasis on *Ostreopsis* species. *Harmful Algae* 32:1–10.
- Selina, M. S. & Orlova, T. Y. 2010. First occurrence of the genus *Ostreopsis* (Dinophyceae) in the Sea of Japan. *Bot. Mar.* 53:243–9.
- Shears, N. T. & Ross, P. M. 2009. Blooms of benthic dinoflagellates of the genus *Ostreopsis*; an increasing and ecologically important phenomenon on temperate reefs in New Zealand and worldwide. *Harmful Algae* 8:916–25.
- Strickland, J. D. H. & Parsons, T. R. 1968. A practical handbook of seawater analysis. *J. Fish. Res. Board Can.* 167:1–310.
- Tamura, K., Stecher, G., Peterson, D., Filipiński, A. & Kumar, S. 2013. MEGA6: Molecular Evolutionary Genetics Analysis version 6.0. *Mol. Biol. Evol.* 30:2725–9.
- Taniyama, S., Arakawa, O., Terada, M., Nishio, S., Takatani, T., Mahmud, Y. & Noguchi, T. 2003. *Ostreopsis* sp., a possible origin of palytoxin (PTX) in parrotfish *Scarus oviifrons*. *Toxicon* 42:29–33.
- Tartaglione, L., Mazzeo, A., Dell'Aversano, C., Forino, M., Giusani, V., Capellacci, S., Penna, A. et al. 2015. Chemical, molecular, and eco-toxicological investigation of *Ostreopsis* sp. from Cyprus Island: structural insights into four new ovatoxins by LC-HRMS/MS. *Anal. Bioanal. Chem.* ???:1–18.
- Tawong, W., Nishimura, T., Sakanari, H., Sato, S., Yamaguchi, H. & Adachi, M. 2014. Distribution and molecular phylogeny of the dinoflagellate genus *Ostreopsis* in Thailand. *Harmful Algae* 37:160–71.
- Thronsen, J. 1978. Preservation and storage. In Sourmia, A. [Ed.] *Phytoplankton Manual. Monographs on Oceanographic Methodology* 6. UNESCO, Paris, pp. 69–74.
- Tichadou, L., Glaizal, M., Armengaud, A., Gossel, H., Lemee, R., Kantin, R., Lasalle, J. L., Drouet, G., Rambaud, L., Malfait, P. & de Haro, L. 2010. Health impact of unicellular algae of the *Ostreopsis* genus blooms in the Mediterranean Sea: experience of the French Mediterranean coast surveillance network from 2006 to 2009. *Clin. Toxicol.* 48:839–44.
- Tillmann, U., Elbraechter, M., Krock, B., John, U. & Cembella, A. 2009. *Azadinium spinosum* gen. et sp. nov. (Dinophyceae) identified as a primary producer of azaspiracid toxins. *Eur. J. Phycol.* 44:63–79.
- Tosteson, T. R. 1995. The diversity and origins of toxins in ciguatera fish poisoning. *P. R. Health Sci. J.* 14:117–29.
- Totti, C., Accoroni, S., Cerino, F., Cucchiari, E. & Romagnoli, T. 2010. *Ostreopsis ovata* bloom along the Conero Riviera (northern Adriatic Sea): relationships with environmental conditions and substrata. *Harmful Algae* 9:233–9.
- Turki, S. 2005. Distribution of toxic dinoflagellates along the leaves of seagrass *Posidonia oceanica* and *Cymodocea nodosa* from the Gulf of Tunis. *Cah. Biol. Mar.* 46:29–34.
- Turki, S., Harzallah, A. & Sammari, C. 2006. Occurrence of harmful dinoflagellates in two different Tunisian ecosystems: the lake of Bizerte and the Gulf of Gabes. *Cah. Biol. Mar.* 47:253–9.
- Uchida, H., Taira, Y. & Yasumoto, T. 2013. Structural elucidation of palytoxin analogs produced by the dinoflagellate *Ostreopsis ovata* IK2 strain by complementary use of positive and negative ion liquid chromatography/quadrupole time-of-flight mass spectrometry. *Rapid Commun. Mass Sp.* 27:1999–2008.
- Vila, M., Garcés, E. & Masó, M. 2001. Potentially toxic epiphytic dinoflagellate assemblages on macroalgae in the NW Mediterranean. *Aquat. Microb. Ecol.* 26:51–60.
- Yasumoto, T., Seino, N., Murakami, Y. & Murata, M. 1987. Toxins produced by benthic dinoflagellates. *Biol. Bull.* 172:128–31.

Author Query Form

Journal: JPY

Article: 12464-16-103

Dear Author,

During the copy-editing of your paper, the following queries arose. Please respond to these by marking up your proofs with the necessary changes/additions. Please write your answers on the query sheet if there is insufficient space on the page proofs. Please write clearly and follow the conventions shown on the attached corrections sheet. If returning the proof by fax do not write too close to the paper's edge. Please remember that illegible mark-ups may delay publication.

Many thanks for your assistance.

Query reference	Query	Remarks
1	AUTHOR: Please confirm that given names (red) and surnames/family names (green) have been identified correctly.	
2	AUTHOR: García-Altres et al. 2014 has not been included in the Reference List, please supply full publication details.	
3	AUTHOR: Accoroni et al. 2014 has not been included in the Reference List, please supply full publication details.	
4	AUTHOR: Coat, 2002 has been changed to Coats 2002 so that this citation matches the Reference List. Please confirm that this is correct.	
5	AUTHOR: Please give manufacturer information for Zeiss Axiovert 135: company name, town, state (if USA), and country.	
6	AUTHOR: Please give manufacturer information for Wild M40: company name, town, state (if USA), and country.	
7	AUTHOR: Please give manufacturer information for Motic BA 400: company name, town, state (if USA), and country.	
8	AUTHOR: Please give manufacturer information for Polaron CPD 7501: company name, town, state (if USA), and country.	
9	AUTHOR: Please provide city for Qiagen.	
10	AUTHOR: Ronquist and Huelsenbeck 2003 has been changed to Ronquist and Huelsenbeck 2003 so that this citation matches the Reference List. Please confirm that this is correct.	
11	AUTHOR: Please provide city and state for Agilent.	
12	AUTHOR: David et al. 2010 has not been included in the Reference List, please supply full publication details.	
13	AUTHOR: Figures 8, 9 and 7 have been changed to Figures 7, 8, and 9. Similar changes are made in text also. Please check.	
14	AUTHOR: Escalera et al. (2015) has not been included in the Reference List, please supply full publication details.	
15	AUTHOR: Dell'Aversano et al. 2014 has been changed to Dell'Aversano et al. 2015 so that this citation matches the Reference List. Please confirm that this is correct.	

16	AUTHOR: Parson et al. 2012 has been changed to Parsons et al. 2012 so that this citation matches the Reference List. Please confirm that this is correct.	
17	AUTHOR: Please provide publisher name for reference Holmes et al. (1988).	
18	AUTHOR: Parsons and Preskitt (2007) has not been cited in the text. Please indicate where it should be cited; or delete from the Reference List.	
19	AUTHOR: Penna and Galluzzi (2013) has not been cited in the text. Please indicate where it should be cited; or delete from the Reference List.	
20	AUTHOR: Please provide volume number for reference Tartaglione et al. (2015).	
21	AUTHOR: Figure 1 has been saved at a low resolution of 305 dpi. Please resupply at 600 dpi. Check required artwork specifications at http://authorservices.wiley.com/bauthor/illustration.asp	
22	AUTHOR: Figure 11 is of poor quality. Please check required artwork specifications at http://authorservices.wiley.com/bauthor/illustration.asp	